3.3. Comparison of intracellular cytokine production between CSF cells and PBL

Representative staining patterns for the cytokines in each group are shown in Fig. 3. CSF cells showed a significantly higher proportion of IFN-γ^+ IL-4$^-$ CD4$^+$ T cells than in PBL in CIDP patients (p=0.0051), VN (p=0.0117) and OND patients (p=0.0022; Fig. 4). IFN-γ^- IL-4$^+$ CD4$^+$ T cell percentages were significantly lower in CSF cells than in PBL in VN patients (p=0.0421) and OND patients (p=0.0342), and also tended to be lower in CIDP patients (p=0.0745). Thus, the intracellular IFN-γ/IL-4 ratio (IFN-γ^+ IL-4$^-$ CD4$^+$ T cell percentage divided by IFN-γ^- IL-4$^+$ CD4$^+$ T cell percentage) was significantly higher in CSF cells than in PBL in CIDP patients (p=0.0051), VN (p=0.0117) and OND patients (p=0.0029). IFN-γ^+ IL-4$^+$ cell percentages were significantly greater in CSF cells than in PBL in CIDP patients (p=0.0284), VN (p=0.0117) and OND patients (p=0.0229).

3.4. Comparison of intracellular cytokine production of CSF cells and PBL among diseases

In CSF cells, IFN-γ^+ IL-4$^-$ cell percentages in CIDP patients showed clustering in the high ranges, while those in VN patients were distributed over a wide range (Fig. 4). Thus, IFN-γ^+ IL-4$^-$ cell percentages were markedly increased in CIDP compared with OND patients (p=0.0008), but not in

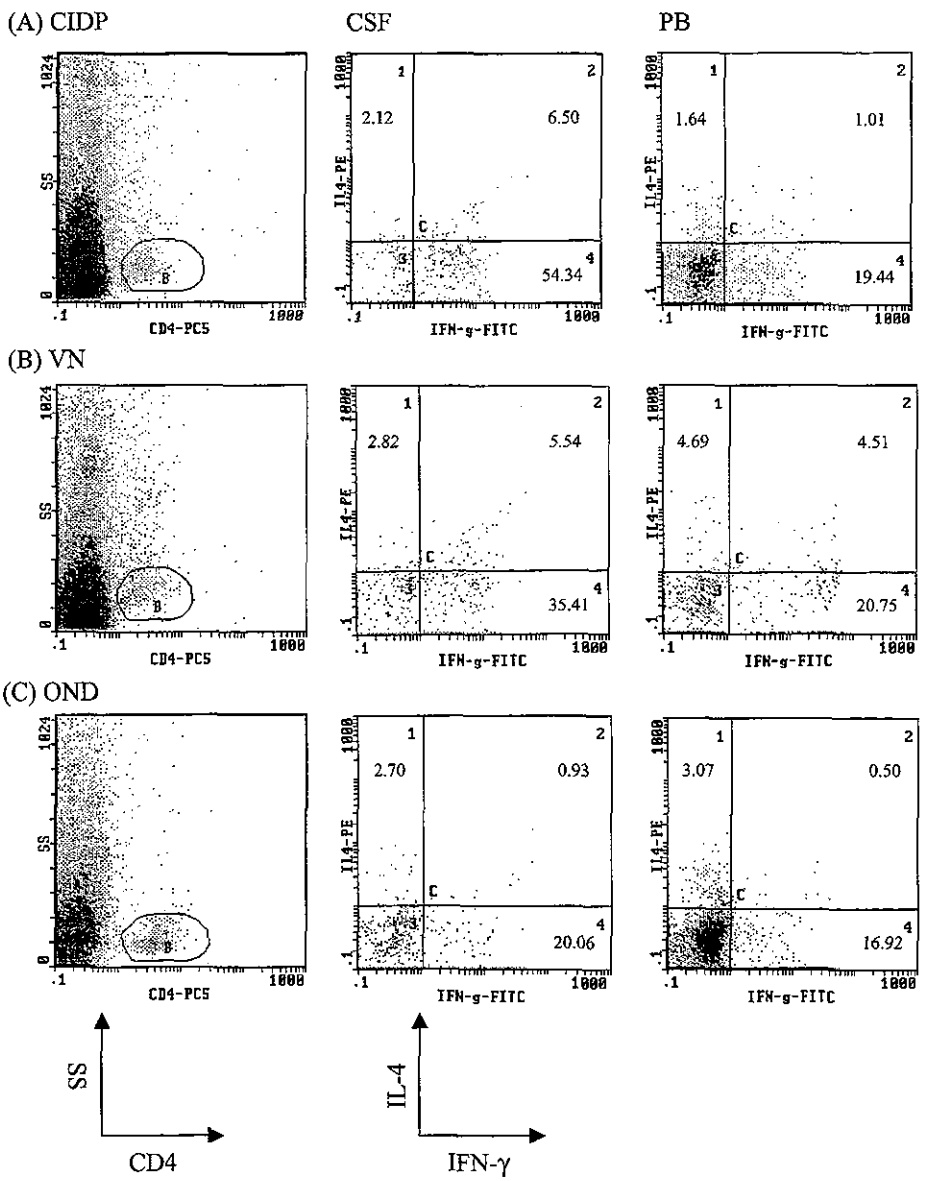

Fig. 3. Representative staining patterns of the intracellular cytokines in CSF CD4$^+$ T cells and peripheral blood (PB) CD4$^+$ T cells from CIDP, VN and OND patients. (A) A 59-year-old patient with CIDP. (B) A 51-year-old patient with VN. (C) A 52-year-old patient with amyotrophic lateral sclerosis. Note the increase in IFN-γ^+ IL-4$^-$ CD4$^+$ T cells in the CIDP CSF cells compared with OND.

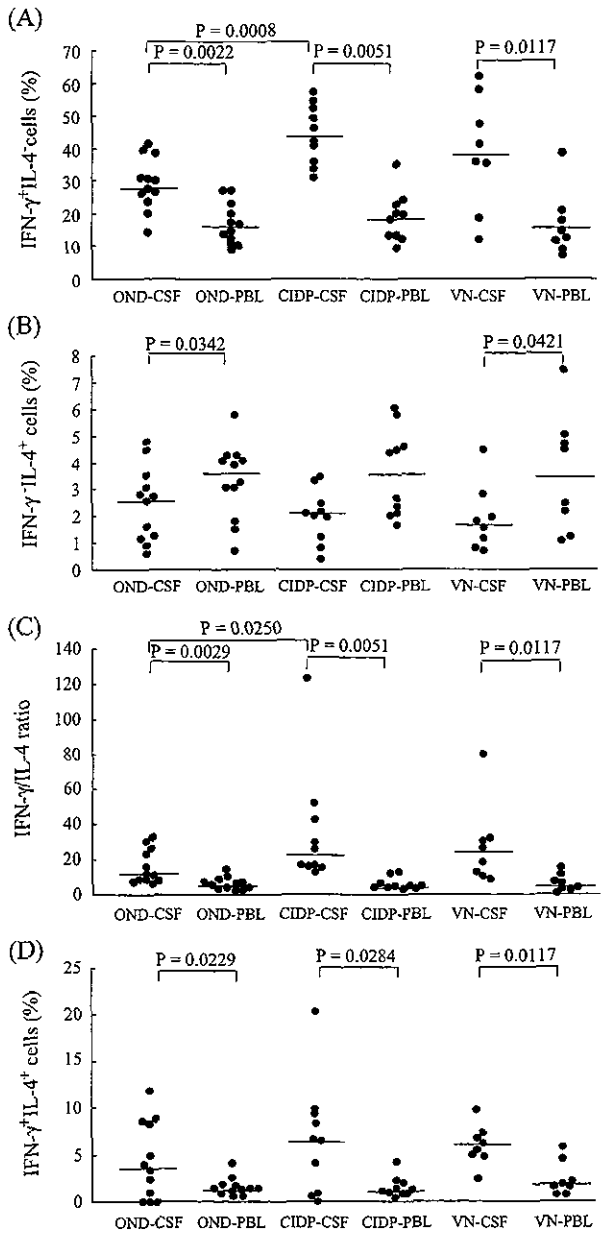

Fig. 4. Intracellular cytokine production patterns of CSF $CD4^+$ T cells in CIDP, VN and OND. (A) IFN-γ^+ IL-4^- $CD4^+$ T cell percentages. (B) IFN-γ^- IL-4^+ $CD4^+$ T cell percentages. (C) Intracellular IFN-γ/IL-4 ratios in $CD4^+$ T cells. (D) IFN-γ^+ IL-4^+ $CD4^+$ T cell percentages.

VN patients, while in PBL, the percentages did not differ significantly among the diseases. IFN-γ^- IL-4^+ cell percentages were not significantly different among the groups in either CSF cells or PBL. Thus, the intracellular IFN-γ/IL-4 ratio was significantly increased in CSF cells in CIDP compared with OND patients (p=0.0250). The ratios in CSF in VN patients, and in PBL in either CIDP or VN patients were not significantly different compared with OND patients. The proportions of IFN-γ^+ IL-4^+ cells in either CSF cells or PBL were not significantly different among the groups.

3.5. Correlation between clinical parameters and intra- and extracellular cytokine levels in CIDP patients

Both IL-17 and IL-8 in CSF supernatant showed significant positive correlation with CSF protein concentrations (r=0.468, p=0.0027 and r=0.579, p=0.0022, respectively; Fig. 5). CIDP patients with increased CSF protein levels at examination had significantly higher levels

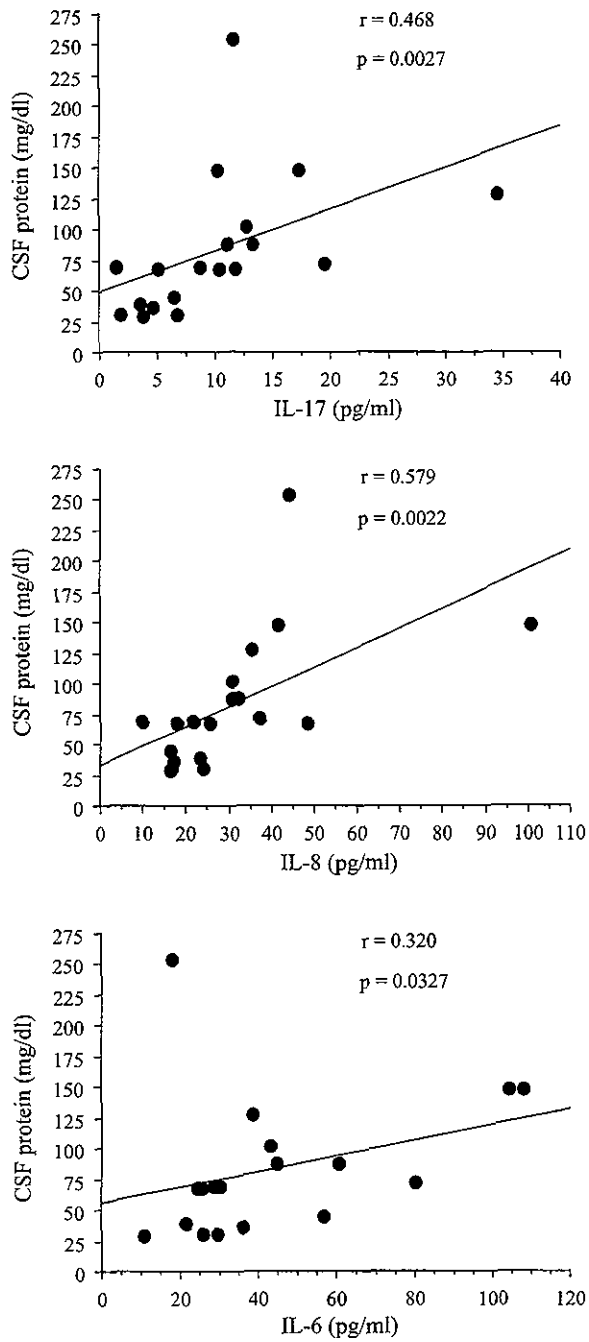

Fig. 5. Correlation between IL-17, IL-8 and IL-6 levels in CSF supernatant and CSF protein concentration. Both IL-17 and IL-8 in CSF supernatant showed a strong positive correlation with CSF protein concentration, while IL-6 showed a weak correlation with CSF protein levels.

of IL-17 and IL-8 than those without the protein increase (12.5±7.83 vs. 4.21±1.75 for the mean±S.D. and 11.39 vs. 3.94 for the median, p=0.0095 in IL-17, and 35.31±21.88 vs. 19.57±3.79 and 31.88 vs. 17.33, p=0.0464 in IL-8). IL-6 levels also showed a weak correlation with CSF protein levels (r=0.320, p=0.0327), and IL-6 levels in CSF tended to be higher in CIDP patients with increased CSF protein levels than in those without the increase (49.4±29.54 vs. 24.83±9.52 and 41.16 vs. 25.85, p=0.0641). In CSF cells of CIDP patients, IVIG nonresponders showed significantly lower IFN-γ^- IL-4^+ $CD4^+$ T cell percentages in CSF at pretreatment than responders (p=0.0105), and the intracellular IFN-γ/IL-4 ratio also tended to be higher in nonresponders than responders (p=0.0811; Fig. 6). No other clinical parameters, such as age at onset or at examination, duration of disease, sex, clinical course and Hughes grade, had any significant correlation with intra- and extracellular cytokine amounts in CSF.

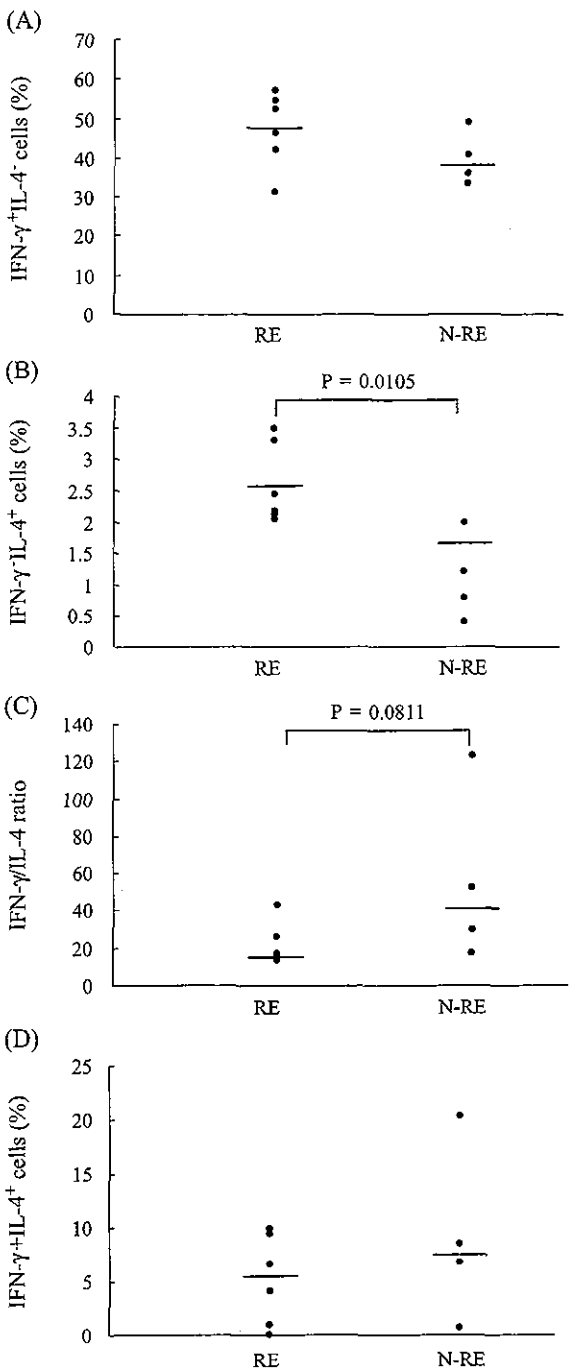

Fig. 6. Comparison of intracellular cytokine production patterns between IVIG responders (RE) and nonresponders (N-RE) in CIDP. (A) IFN-γ^+ IL-4^- $CD4^+$ T cell percentages. (B) IFN-γ^-IL-4^- $CD4^+$ T cell percentages. (C) Intracellular IFN-γ/IL-4 ratios in $CD4^+$ T cells. (D) IFN-γ^+ IL-4^+ $CD4^+$ T cell percentages.

4. Discussion

The present study is the first to demonstrate changes in intracellular cytokine production in CSF cells and changes in secreted cytokine levels in CSF supernatant, by a combined intra- and extracellular cytokine analysis in CIDP and VN. Our method successfully measured the intracellular cytokine production even in the absence of CSF pleocytosis. Cytokine assessment at the cellular level in the CSF has been difficult because of the extreme fragility of CSF cells and their limited numbers. In the current study, even in the absence of CSF pleocytosis, CIDP patients were found to have a marked increase in IFN-γ-producing $CD4^+$ T cells and thus a greater Th1 shift in the CSF compartment than OND patients, which coincided with upregulation of type 1 cytokine, IL-17, and downregulation of type 2 cytokines, such as IL-4 and IL-5. In contrast, VN patients showed upregulation of type 2 cytokines, such as IL-6 and IL-10.

Among the cytokines that were elevated in the CSF supernatant in the pretreated patients, IL-17 was upregulated in CIDP patients but not in VN patients. In addition, IL-10 was elevated in VN patients but not in CIDP patients, whereas both IL-6 and IL-8 levels were upregulated in CIDP patients as well as VN patients, suggesting unique roles for IL-17 in CIDP and IL-10 in VN. IL-17 is a potent proinflammatory cytokine produced by a subset of memory $CD4^+$ T cells, mainly Th1 type, on activation [13–15]. IL-17 triggers the local production of downstream cytokines and chemokines, such as IL-6, IL-8, MCP-1 and G-CSF, from a wide variety of cells [13,15,16]. It is possible that increase of IL-6 and IL-8 found in the present study may be triggered by IL-17. In addition, IL-17 stimulates the production of matrix metalloproteinases [17,18], iNOS, NO [19,20] and PGE2 [13,21], which enhance the local inflammatory environment; as shown in rheumatoid arthritis (RA) where high levels of IL-17 in synovial fluid contribute to inflammatory joint destruction [22,23]. In the present study, both IL-17 and IL-8 levels positively correlated with CSF protein concentrations in CIDP patients, which indicates that an increase of those cytokines/chemokines is related to the severity of inflammation in the spinal roots. Both IL-6 and IL-8 are proinflammatory cytokines and contribute to exacerbate various

autoimmune inflammatory diseases, such as rheumatoid arthritis (RA) [24], systemic lupus erythematosus (SLE) [25], ulcerative colitis [26], Crohn's disease [27] and psoriasis [24]. IL-6 induces an acute phase response, activates monocytes [28] and induces other chemokines [29], such as MIP-2, and adhesion molecules [30]; while IL-8 recruits granulocytes and T cells to the local inflammatory sites [31,32]. Therefore, increased IL-6 and IL-8 responses could also contribute to enhance local inflammation in CIDP.

In contrast, type 2 cytokines, IL-4 and IL-5, were downregulated in CSF supernatant only in CIDP patients. IL-7, which was originally described as a growth and differentiation factor for precursor B cells [33] and was later shown to prime human naïve $CD4^+$ T cells for IFN-γ as well as IL-4 [34], was downregulated in CIDP CSF in the present study. The underlying disease process of CIDP appears to cause this cytokine to behave similarly to type 2 cytokines. This finding is similar to those in other organ-specific autoimmune diseases, such as bullous pemphigoid, where IL-7 is downregulated more in the blister fluid than in the sera [35].

IVIG treatment has been shown to be effective in CIDP and can shift the immune balance from the Th1 to the Th2 side [36,37]. Therefore, the beneficial effects of giving IVIG in CIDP are at least partly attributable to the correction of the pathogenic Th1 shift. However, since the nonresponders to IVIG showed significantly lower IFN-γ^- IL-4^+ $CD4^+$ T cells than responders, IVIG does not appear able to overcome the disease process in CIDP patients with markedly depressed Th2 cells in CSF.

Mathey et al. [38] showed that mRNA expression of Th1 cytokines, such as IFN-γ, TNF-α and IL-2, was upregulated in the biopsied sural nerves from CIDP patients. However, in CSF supernatant, IL-2 was barely detectable in any of the diseases examined, and the increases of TNF-α and IFN-γ concentrations were not statistically significant. Although one ELISA study has demonstrated an increase of TNF-α concentrations in CIDP sera in a fraction of patients with grave disability [39], in the present study, only a minority of CIDP patients with grave disease (Hughes grade 4) had very high TNF-α concentrations in CSF. This observation might be explained by the very short half life of TNF-α, i.e., 30 min [40], or alternatively, a distinct subset of CIDP patients may preferentially produce TNF-α. For IFN-γ, intracellular cytokine analysis is superior to extracellular cytokine measurement; probably because intracellular cytokine analysis measures the preprogrammed potential of cytokine production in each cell directly, and thus the amounts are not diluted by other factors, such as large volumes of continually replacing CSF.

Although we previously reported that Th2 cells are also increased in peripheral blood in some CIDP patients by intracellular cytokine analysis [41], Th1 shift is evident in CSF cells. It is possible that Th1 cells move from peripheral blood to nerves beyond the BNB, and CSF cells more sensitively reflect the pathological process occurring within the BNB in CIDP.

In the present study, IL-6, IL-8 and IL-10 levels were found to be upregulated in CSF supernatant in VN patients; a group in which CSF cytokine changes have never been reported. In addition, acting as a proinflammatory cytokine, IL-6 increases fibrinogen amounts [42] and platelet number [43], and increases blood viscosity through the induction of hepatic acute phase response [24]. Therefore, it is possible that an increase of IL-6 exacerbates vasculitis-related ischemia of the peripheral nerves. Furthermore, both IL-6 and IL-10 can enhance autoantibody production [24,25,44–46]. Although the increase of IL-10 in VN could be the result of the host's efforts to counteract inflammation since IL-10 works as anti-inflammatory cytokine [47], IL-10 itself is regarded as an exacerbating factor in vasculitic disorders, such as SLE [25,48], RA [46], Sjögren's syndrome [44] and Wegener's granulomatosis [45], through enhanced autoantibody production. As immunoglobulins, complements and immune complexes are deposited in the vessel wall in VN [3,49], enhanced IL-6 and IL-10 responses in CSF may act as exacerbating factors in this condition.

Since no increase of intracellular IFN-γ/IL-4 ratio in CSF cells was observed in VN patients, the commitment of Th1 cells may be less important in VN than in CIDP. However, intracellular IFN-γ^+ IL-4^- $CD4^+$ cell percentages in VN CSF were distributed over a wide range, which is in contrast to the clustering observed in the high ranges in CIDP patients. This indicates the heterogeneous nature of VN and further investigation of CSF intracellular cytokine analyses together with further subclassification of VN is required.

In conclusion, our combined multiplexed fluorescent bead-based immunoassay and intracellular cytokine analysis of CSF successfully demonstrated the upregulation of Th1 and downregulation of Th2 cytokines, increased IFN-γ producing $CD4^+$ T cells in CIDP patients and the upregulation of some Th2 cytokines in VN patients. Thus, we propose that IL-4, IL-5, IL-6, IL-7, IL-8, IL-10 and IL-17 are clinically useful sets of cytokines for CSF immune monitoring by multiplexed fluorescent bead-based immunoassay.

Acknowledgements

This work was supported in part by a Neuroimmunological Disease Research Committee grant, a Research on Brain Science grant from the Ministry of Health and Welfare, Japan, and Grants 12470142, 12557060 and 12877097 from the Ministry of Education, Science, Sports and Culture, Japan.

References

[1] Matsumuro K, Izumo S, Umehara F, Osame M. Chronic inflammatory demyelinating polyneuropathy: histological and immunopathological studies on biopsied sural nerves. J Neurol Sci 1994;127:170–8.
[2] Rizzuto N, Morbin M, Cavallaro T, Ferrari S, Fallahi M, Galiazzo Rizzuto S. Focal lesions area feature of chronic inflammatory

demyelinating polyneuropathy (CIDP). Acta Neuropathol (Berl) 1998; 96:603–9.
[3] Davies L, Spies JM, Pollard JD, McLeod JG. Vasculitis confined to peripheral nerves. Brain 1996;119:1441–8.
[4] Kieseier BC, Tani M, Mahad D, Oka N, Ho T, Woodroofe N, et al. Chemokines and chemokine receptors in inflammatory demyelinating neuropathies: a central role for IP-10. Brain 2002;125:823–34.
[5] Mahad DJ, Howell SJL, Woodroofe MN. Expression of chemokines in cerebrospinal fluid and serum of patients with chronic inflammatory demyelinating polyneuropathy. J Neurol Neurosurg Psychiatry 2002; 73:320–3.
[6] Sivieri S, Ferrarini AM, Lolli F, Matà S, Pinto F, Tavolato B, et al. Cytokine pattern in the cerebrospinal fluid from patients with GBS and CIDP. J Neurol Sci 1997;147:93–5.
[7] Maimone D, Annunziata P, Simone IL, Livrea P, Guazzi GC. Interleukin-6 levels in the cerebrospinal fluid and serum of patients with Guillain–Barré syndrome and chronic inflammatory demyelinating polyradiculoneuropathy. J Neuroimmunol 1993;47:55–61.
[8] Vignali DAA. Multiplexed particle-based flow cytometric assays. J Immunol Methods 2000;243:243–55.
[9] de Jager W, te Velthuis H, Prakken BJ, Kuis W, Rijkers GT. Simultaneous detection of 15 human cytokines in a single sample of stimulated peripheral blood mononuclear cells. Clin Diagn Lab Immunol 2003;10:133–9.
[10] Report from an Ad Hoc Subcommittee of the American Academy of Neurology AIDS Task Force. Research criteria for diagnosis of chronic inflammatory demyelinating polyneuropathy (CIDP). Neurology 1991;41:617–8.
[11] Hughes RAC, Newsom-Davis JM, Perkin GD, Pierce JM. Controlled trial prednisolone in acute polyneuropathy. Lancet 1978;2:750–3.
[12] Horiuchi I, Kawano Y, Yamasaki K, Minohara M, Furue M, Taniwaki T, et al. Th1 dominance in HAM/TSP and the optico-spinal form of multiple sclerosis versus Th2 dominance in mite antigen-specific IgE myelitis. J Neurol Sci 2000;172:17–24.
[13] Fossiez F, Djossou O, Chomarat P, Flores-Romo L, Ait-Yahia S, Maat C, et al. T cell interleukin-17 induces stromal cells to produce proinflammatory and hematopoietic cytokines. J Exp Med 1996;183: 2593–603.
[14] Schwarzenberger P, Huang W, Ye P, Oliver P, Manuel M, Zhang Z, et al. Requirement of endogenous stem cell factor and granulocyte-colony-stimulating factor for IL-17-mediated granulopoiesis. J Immunol 2000;164:4783–9.
[15] Aggarwal S, Gurney AL. IL-17: prototype member of an emerging cytokine family. J Leukoc Biol 2002;71:1–8.
[16] Hwang S-Y, Kim J-Y, Kim K-W, Park M-K, Moon Y, Kim W-U. IL-17 induces production of IL-6 and IL-8 in rheumatoid arthritis synovial fibroblasts via NF-κB- and PI3-kinase/Akt-dependent pathways. Arthritis Res Ther 2004;6:R120–8.
[17] Jovanovic DV, Martel-Pelletier J, Di Battista JA, Mineau F, Jolicoeur F-C, Benderdour M, et al. Stimulation of 92-kd gelatinase (matrix metalloproteinase 9) production by interleukin-17 in human monocyte/macrophages: a possible role in rheumatoid arthritis. Arthritis Rheum 2000;43:1134–44.
[18] Prause O, Bozinovski S, Anderson GP, Lindén A. Increased matrix metalloproteinase-9 concentration and activity after stimulation with interleukin-17 in mouse airways. Thorax 2004;59:313–7.
[19] Trajkovic V, Stosic-Grujicic S, Samardzic T, Markovic M, Miljkovic D, Ramic Z, et al. Interleukin-17 stimulates inducible nitric oxide synthase activation in rodent astrocytes. J Neuroimmunol 2001;119:183–91.
[20] Miljkovic D, Trajkovic V. Inducible nitric oxide synthase activation by interleukin-17. Cytokine Growth Factor Rev 2004;15:21–32.
[21] Kotake S, Udagawa N, Takahashi N, Matsuzaki K, Itoh K, Ishiyama S, et al. IL-17 in synovial fluids from patients with rheumatoid arthritis is a potent stimulator of osteoclastogenesis. J Clin Invest 1999;103:1345–52.
[22] Ziolkowska M, Koc A, Luszczykiewicz G, Ksiezopolska-Pietrzak K, Klimczak E, Chwalinska-Sadowska H, et al. High levels of IL-17 in rheumatoid arthritis patients: IL-15 triggers in vitro IL-17 production via cyclosporin A-sensitive mechanism. J Immunol 2000;164:2832–8.
[23] Dudler J, Renggli-Zulliger N, Busso N, Lotz M, So A. Effect of interleukin 17 on proteoglycan degradation in murine knee joints. Ann Rheum Dis 2000;59:529–32.
[24] Ishihara K, Hirano T. IL-6 in autoimmune disease and chronic inflammatory proliferative disease. Cytokine Growth Factor Rev 2002;13:357–68.
[25] Cross JT, Benton HP. The roles of interleukin-6 and interleukin-10 in B cell hyperactivity in systemic lupus erythematosus. Inflamm Res 1999;48:255–61.
[26] Larsen TB, Nieslsen JN, Fredholm L, Lund ED, Brandslund I, Munkholm P, et al. Platelets and anticoagulant capacity in patients with inflammatory bowel disease. Pathophysiol Haemost Thromb 2002;32:92–6.
[27] Ito H. IL-6 and Crohn's disease. Curr Drug Targets Inflamm Allergy 2003;2:125–30.
[28] Sebbag M, Parry SL, Brennan FM, Feldmann M. Cytokine stimulation of T lymphocytes regulates their capacity to induce monocyte production of tumor necrosis factor-alpha, but not interleukin-10: possible relevance to pathophysiology of rheumatoid arthritis. Eur J Immunol 1997;27:624–32.
[29] McLoughlin RM, Hurst SM, Nowell MA, Harris DA, Horiuchi S, Morgan LW, et al. Differential regulation of neutrophil-activating chemokines by IL-6 and its soluble receptor isoforms. J Immunol 2004;172:5676–83.
[30] Dahlman-Ghozlan K, Ortonne J-P, Heilborn JD, Stephansson E. Altered tissue expression pattern of cell adhesion molecules, ICAM-1, E-selectin and VCAM-1, in bullous pemphigoid during methotrexate therapy. Exp Dermatol 2004;13:65–9.
[31] Chertov O, Michiel DF, Xu L, Wang JM, Tani K, Murphy WJ, et al. Identification of defensin-1, defensin-2, and CAP37/azurocidin as T-cell chemoattractant proteins released from interleukin-8-stimulated neutrophils. J Biol Chem 1996;271:2935–40.
[32] Gesser B, Lund M, Lohse N, Vestergaard C, Matsushima K, Sindet-Pedersen S, et al. IL-8 induces T cell chemotaxis, suppresses IL-4, and up-regulates IL-8 production by $CD4^+$ T cells. J Leukoc Biol 1996;59:407–11.
[33] Morrissey PJ, Goodwin RG, Nordan RP, Anderson D, Grabstein KH, Cosman D, et al. Recombinant interleukin 7, pre-B cell growth factor, has costimulatory activity on purified mature T cells. J Exp Med 1989;169:707–16.
[34] van Roon JAG, Glaudemans CAFM, Bijlsma JWJ, Lafeber FPJG. Differentiation of naïve $CD4^+$ T cells towards T helper 2 cells is not impaired in rheumatoid arthritis patients. Arthritis Res Ther 2003; 5:R269–76.
[35] Giacalone B, D'Auria L, Bonifati C, Riccardi E, Mussi A, D'Agosto G, et al. Decreased interleukin-7 and transforming growth factor-beta1 levels in blister fluids as compared to the respective serum levels in patients with bullous pemphigoid. Opposite behavior of TNF-alpha, interleukin-4 and interleukin-10. Exp Dermatol 1998;7: 157–61.
[36] Ochi K, Kohriyama T, Higaki M, Ikeda J, Harada A, Nakamura S. Changes in serum macrophage-related factors in patients with chronic inflammatory demyelinating polyneuropathy caused by intravenous immunoglobulin therapy. J Neurol Sci 2003;208:43–50.
[37] Dalakas MC. Mechanisms of action of IVIg and therapeutic considerations in the treatment of acute and chronic demyelinating neuropathies. Neurology 2002;59:S13–21.
[38] Mathey EK, Pollard JD, Armati PJ. TNFα, IFNγ and IL-2 mRNA expression in CIDP sural nerve biopsies. J Neurol Sci 1999;163: 47–52.
[39] Misawa S, Kuwabara S, Mori M, Kawaguchi N, Yoshiyama Y, Hattori T. Serum levels of tumor necrosis factor-a in chronic inflammatory demyelinating polyneuropathy. Neurology 2001;56:666–9.
[40] Li Y-P, Pei Y-Y, Zhou Z-H, Zhang X-Y, Gu Z-H, Ding J, et al. PEGylated recombinant human tumor necrosis factor alpha:

pharmacokinetics and anti-tumor effects. Biol Pharm Bull 2001; 24:666–70.
[41] Horiuchi I, Ochi H, Murai H, Osoegawa M, Minohara M, Furuya H, et al. Th2 shift in mononeuritis multiplex and increase of Th2 cells in chronic inflammatory demyelinating polyneuropathy: an intracellular cytokine analysis. J Neurol Sci 2001;193:49–52.
[42] Raj DSC, Dominic EA, Wolfe R, Shah VO, Bankhurst A, Zager PG, et al. Coordinated increase in albumin, fibrinogen, and muscle protein synthesis during hemodialysis: role of cytokines. Am J Physiol Endocrinol Metab 2004;286:E658–64.
[43] Ertenli I, Kiraz S, Öztürk MA, Haznedaroğlu IC, Çelik İ, Çalgüneri M. Pathologic thrombopoiesis of rheumatoid arthritis. Rheumatol Int 2003;23:49–60.
[44] Anaya JM, Correa PA, Herrera M, Eskdale J, Gallagher G. Interleukin-10 (IL-10) influences autoimmune response in primary Sjögren's syndrome and is linked to IL-10 gene polymorphism. J Rheumatol 2002;29:1874–6.
[45] Zhou Y, Giscombe R, Huang D, Lefvert AK. Novel genetic association of Wegener's granulomatosis with the interleukin-10 gene. J Rheumatol 2002;29:317–20.
[46] Lard LR, van Gaalen FA, Schonkeren JJ, Pieterman EJ, Stoeken G, Vos K, et al. Association of the-2849 interleukin-10 promoter polymorphism with autoantibody production and joint destruction in rheumatoid arthritis. Arthritis Rheum 2003;48:1841–8.
[47] Li M-C, He S-H. IL-10 and its related cytokines for treatment of inflammatory bowel disease. World J Gastroenterol 2004;10:620–5.
[48] Willeke P, Schotte H, Erren M, Schlüter B, Mickholz E, Domschke W, et al. Concomitant reduction of disease activity and IL-10 secreting peripheral blood mononuclear cells during immunoadsorption in patients with active systemic lupus erythematosus. Cell Mol Biol 2002;48:323–9.
[49] Hattori N, Ichimura M, Nagamatsu M, Li M, Yamamoto K, Kumazawa K, et al. Clinicopathological features of Churg–Strauss syndrome-associated neuropathy. Brain 1999;122:427–39.

Prevention of Experimental Autoimmune Encephalomyelitis by Transfer of Embryonic Stem Cell-Derived Dendritic Cells Expressing Myelin Oligodendrocyte Glycoprotein Peptide along with TRAIL or Programmed Death-1 Ligand[1]

Shinya Hirata, Satoru Senju, Hidetake Matsuyoshi, Daiki Fukuma, Yasushi Uemura, and Yasuharu Nishimura[2]

Experimental autoimmune encephalomyelitis (EAE) is caused by activation of myelin Ag-reactive CD4$^+$ T cells. In the current study, we tested a strategy to prevent EAE by pretreatment of mice with genetically modified dendritic cells (DC) presenting myelin oligodendrocyte glycoprotein (MOG) peptide in the context of MHC class II molecules and simultaneously expressing TRAIL or Programmed Death-1 ligand (PD-L1). For genetic modification of DC, we used a recently established method to generate DC from mouse embryonic stem cells (ES cells) in vitro (ES-DC). ES cells were sequentially transfected with an expression vector for TRAIL or PD-L1 and an MHC class II-associated invariant chain-based MOG epitope-presenting vector. Subsequently, double-transfectant ES cell clones were induced to differentiate to ES-DC, which expressed the products of introduced genes. Treatment of mice with either of the double-transfectant ES-DC significantly reduced T cell response to MOG, cell infiltration into spinal cord, and the severity of MOG peptide-induced EAE. In contrast, treatment with ES-DC expressing MOG alone, irrelevant Ag (OVA) plus TRAIL, or OVA plus PD-L1, or coinjection with ES-DC expressing MOG plus ES-DC-expressing TRAIL or PD-L1 had no effect in reducing the disease severity. In contrast, immune response to irrelevant exogenous Ag (keyhole limpet hemocyanin) was not impaired by treatment with any of the genetically modified ES-DC. The double-transfectant ES-DC presenting Ag and simultaneously expressing immune-suppressive molecules may well prove to be an effective therapy for autoimmune diseases without inhibition of the immune response to irrelevant Ag. *The Journal of Immunology,* 2005, 174: 1888–1897.

Currently, corticosteroids and other immune suppressants are commonly used for treatment of subjects with autoimmune diseases. The medication with these drugs often leads to systemic immune suppression and consequent opportunistic infections. Thus, it is desirable to develop a therapeutic means to down-modulate immune responses in an Ag-specific manner without causing systemic immune suppression.

Experimental autoimmune encephalomyelitis (EAE),[3] an animal model for human multiple sclerosis, is characterized by neurological impairment resulting from demyelination in the CNS caused by myelin Ag-reactive CD4$^+$ T cells. This disease model is induced by immunization with myelin Ags such as myelin oligodendrocyte glycoprotein (MOG). In the current study, we wanted to try to prevent MOG-induced EAE by treatment of mice with genetically modified dendritic cells (DC). We generated double-transfectant DC presenting MOG peptide in the context of MHC class II molecules and simultaneously expressing molecules with T cell-suppressive property. We tested a strategy to down-modulate the immune response in an Ag-specific manner by in vivo transfer of such genetically modified DC to prevent development of the disease.

For efficient presentation of MOG peptide in the context of MHC class II molecules, we used a previously devised expression vector in which cDNA for human MHC class II-associated invariant chain (Ii) was mutated to contain antigenic peptide in the class II-associated Ii peptide (CLIP) region (1). An epitope inserted in this vector is efficiently presented in the context of coexpressed MHC class II molecules (2). Because they are molecules with a T cell-suppressive property, we tested TRAIL and Programmed Death-1 ligand (PD-L1). TRAIL, a member of the TNF superfamily, is constitutively expressed in a variety of cell types, including lymphocytes, NK cells, and neural cells (3, 4). TRAIL$^{-/-}$ mice are hypersensitive to collagen-induced arthritis and streptozotocin-induced diabetes (5). PD-L1, a ligand for PD-1 and member of the CD28/CTLA-4 family, is expressed on DC, IFN-γ-treated monocytes, activated T cells, placental trophoblasts, myocardial endothelium, and cortical thymic epithelial cells (6, 7). PD-1$^{-/-}$ mice spontaneously develop a lymphoproliferative/autoimmune disease, a lupus-like disease, arthritis, and cardiomyopathy (8, 9). Thus, abrogation of either of these two molecules make mice autoimmune prone, suggesting that these molecules play significant roles

Department of Immunogenetics, Graduate School of Medical Sciences, Kumamoto University, Kumamoto, Japan

Received for publication May 20, 2004. Accepted for publication December 8, 2004.

The costs of publication of this article were defrayed in part by the payment of page charges. This article must therefore be hereby marked *advertisement* in accordance with 18 U.S.C. Section 1734 solely to indicate this fact.

[1] This work was supported in part by Grants-in-Aid 12213111, 14370115, 14570421, and 14657082 from the Ministry of Education, Science, Technology, Sports, and Culture, Japan, and a Research Grant for Intractable Diseases from Ministry of Health, Labour and Welfare, Japan, and grants from the Tokyo Biochemical Research Foundation and Uehara Memorial Foundation, and by funding from Meiji Institute of Health Science.

[2] Address correspondence and reprint requests to Dr. Yasuharu Nishimura, Department of Immunogenetics, Graduate School of Medical Sciences, Kumamoto University, Honjo 1-1-1, Kumamoto 860-8556, Japan. *E-mail address: mxnishim@gpo.kumamoto-u.ac.jp*

[3] Abbreviations used in this paper: EAE, experimental autoimmune encephalomyelitis; MOG, myelin oligodendrocyte glycoprotein; DC, dendritic cell; Ii, invariant chain; CLIP, class II-associated Ii peptide; PD-L1, Programmed Death-1 ligand; ES cell, embryonic stem cell; ES-DC, ES cell-derived DC; PLP, myelin proteolipid protein; MBP, myelin basic protein; IRES, internal ribosomal entry site; PCC, pigeon cytochrome *c*; KLH, keyhole limpet hemocyanin.

0022-1767/05/$02.00

in maintaining immunological self-tolerance in physiological situations (10–18).

For introduction of multiple expression vectors into DC, we used a method for embryonic stem cell (ES cell)-mediated genetic modification of DC. Recently, we and another group established culture procedures to generate DC from mouse ES cells (2, 19). ES cell-derived DC (esDC or ES-DC) have the capacity comparable to bone marrow-derived DC to process and present protein Ags to T cells, stimulate naive T cells, and migrate to lymphoid organs in vivo (20, 21). A recent study using the method revealed the role of Notch signaling in differentiation of DC (22). For generation of genetically modified ES-DC, ES cells were transfected with expression vectors, and subsequently transfectant ES cell clones were induced to differentiate to DC, which expressed the products of introduced genes. Introduction of multiple exogenous genes by sequential transfection can readily be done with vectors bearing different selection markers (20).

In this study, we report that treatment of mice with ES-DC presenting MOG peptide in the context of MHC class II and simultaneously expressing TRAIL or PD-L1 significantly reduced the severity of EAE induced by immunization with the MOG peptide.

Materials and Methods

Mice

CBA, and C57BL/6 mice obtained from CLEA Japan or Charles River were kept under specific pathogen-free conditions. Male CBA and female C57BL/6 mice were mated to generate F_1 (CBF_1) mice, and all in vivo experiments were done using CBF_1 mice, syngeneic to TT2 ES cells. Mouse experiments met with approval by Animal Research Committee of Kumamoto University.

Peptides, protein, cell lines, and cytokines

The mouse MOG p35–55 (MEVGWYRSPFSRVVHLYRNGK), mouse myelin proteolipid protein (PLP) p190–209 (SKTSASIGSLCADARM YGVL), and mouse myelin basic protein (MBP) p35–47 (TGILDSI GRFFSG), were synthesized using the F-moc method on an automatic peptide synthesizer (PSSM8; Shimadzu) and purified using HPLC (23–25). Bovine MBP was purchased from Sigma-Aldrich. The ES cell line, TT2, derived from CBF_1 blastocysts, and the M-CSF-defective bone marrow-derived stromal cell line, OP9, were maintained, as described (2). L929, a fibroblast cell line originating from a C3H mouse was purchased from Japan Health Science Foundation (Osaka, Japan). Recombinant mouse GM-CSF was kindly provided by Kirin Brewery and was purchased from PeproTech.

Plasmid construction

Mouse *TRAIL* cDNA was prepared by RT-PCR amplification from total RNA of mouse spleen with PCR primers 5′-AACCCTCTAGACCGC CGCCACCATGCCTTCCTCAGGGGCCCTGAA-3′ and 5′-AAAGGGA TATCTTTACTGGTCATTTAGTT-3′. The design of these primers results in cloning of *TRAIL* cDNA downstream of the Kozak sequence (20). The PCR products were subcloned into a pGEM-T-Easy vector (Promega), and cDNA inserts were confirmed by sequencing analysis. cDNA for mouse *PD-L1* was kindly provided by Drs. T. Okazaki and T. Honjo (Department of Medical Chemistry, Kyoto University, Kyoto, Japan) (7). The cDNA fragments for *TRAIL* and *PD-L1* were cloned into pCAG-INeo, a mammalian expression vector driven by a CAG promoter and containing the internal ribosomal entry site (IRES)-neomycin resistance gene cassette, to generate pCAG-TRAIL-INeo or pCAG-PDL1-INeo. To generate a MOG peptide presenting vector, double-stranded oligo DNA encoding the MOG p35–55 epitope, 5′-CCGGTGATGGAAGTTGGTTGGTATCGTT CTCCATTCTCTCGTGTTGTTCATCTTTATCGTAACGGTAAG CTGCCCATGGGAGCT-3′, was inserted into the previously reported human Ii-based epitope-presenting vector, pCI30 (2). The coding region of this construct was transferred to pCAG-IPuro, an expression vector containing the CAG promoter and IRES-puromycin *N*-acetyltransferase gene cassette, to generate pCAG-MOG-IPuro. pCI-PCC is a pigeon cytochrome *c* (PCC) epitope-presenting vector derived from pCI30 (2).

Transfection of ES cells and differentiation of DC from ES cells

Transfection of ES cells and induction of differentiation of ES cells into DC were done as described (2, 20), with some minor modification as follows. The differentiating cells were transferred from OP9 to bacteriological petri dishes without feeder cells on day 10, and cultured in RPMI 1640 medium supplemented with 12% FCS, GM-CSF (500 U/ml), and 2-ME. The floating or loosely adherent cells were recovered from dishes by pipetting on days 17–19 and used for experiments.

RT-PCR to detect transgene products

Total cellular RNA was extracted using a SV Total RNA Isolation kit (Promega). All RNA samples were treated with RNase-free DNase I before reverse transcription to eliminate any contaminating genomic DNA. RT-PCR was done as described (20). The relative quantity of cDNA in each sample was first normalized by PCR for GAPDH. The primer sequences were as follows: *hCD74* (Ii), 5′-CTGACTGACCGCGTTACTCCCACA-3′ and 5′-TTCAGGGGGTCAGCATTCTGGAGC-3′; *TRAIL*, 5′-CTGACTGAC CGCGTTACTCCCACA-3′ and 5′-GAAATGGTGTCCTGAAAGGTTC-3′; *PD-L1*, 5′-CTGACTGACCGCGTTACTCCCACA-3′ and 5′-GCTTGTAG TCCGCACCACCGTAG-3′; and *GAPDH*, 5′-GGAAAGCTGTG GCGTGATG-3′ and 5′-CTGTTGCTGTAGCCGTATTC-3′. The sense-strand primer used for detection of transgene-derived mRNA was corresponding to the 5′ untranslated region included in the vector DNA. PCR products were visualized by ethidium bromide staining after separation over a 2% agarose gel. In one experiment, the level of expression of mRNA for *TGF-β* was detected by RT-PCR. The primer sequences were 5′-ACCATGCCAACTTCTGTCTG-3′ and 5′-CGGGTTGTGTTGGT TGTAGA-3′.

Flow-cytometric analysis

Staining of cells and analysis on a flow cytometer (FACScan; BD Biosciences) was done as described (2). Abs and reagent used for staining were as follows: anti-I-A^b (clone 3JP; mouse IgG2a), R-PE-conjugated-anti-mouse CD11c (clone N148; hamster IgG; Chemicon), R-PE-conjugated anti-mouse CD86 (clone RMMP-2; rat IgG2a; Caltag), FITC-conjugated anti-human CD74 (clone M-B741; mouse IgG2a; BD Pharmingen), FITC-conjugated goat anti-mouse Ig (BD Pharmingen), mouse IgG2a control (clone G155-178; BD Pharmingen), FITC-conjugated mouse IgG2a control (clone G155-178; BD Pharmingen), R-PE-conjugated hamster IgG control (Immunotech), R-PE-conjugated rat IgG2a control (clone LO-DNP-16; Caltag), biotinylated anti-mouse TRAIL (clone N2B2; rat IgG2a; eBioscience), anti-mouse PD-L1 (clone MIH5; rat IgG2a; eBioscience), rat IgG2a (Caltag), biotinylated rat IgG2a (eBioscience), FITC-conjugated anti-rat Ig (BD Pharmingen), and PE conjugated-streptavidin (Molecular Probes; Invitrogen Life Technologies). In some experiments, the DC fraction was gated by forward and side scatters. For detection of apoptosis of splenic $CD4^+$ T cell, Annexin V^{FITC} apoptosis detection kits (BioVision) were used. In brief, spleen cells isolated from mice treated with ES-DC were incubated with FITC-conjugated annexin V and R-PE-conjugated anti-mouse CD4 mAb (clone L3T4; BD Pharmingen), and subsequently analyzed by flow cytometry.

Cytotoxicity assay and proliferation assay of T cells stimulated with anti-CD3 mAb

Standard ^{51}Cr release assay was done as described (4). For proliferation assay of T cells stimulated with anti-CD3 mAb, splenic mononuclear cells were prepared from unprimed CBF_1 mice, and T cells were purified using nylon wool columns. X-ray-irradiated (35 Gy) ES-DC (2×10^4) and the T cells (1×10^5) were seeded into wells of 96-well flat-bottom culture plates precoated with anti-CD3 mAb (145-2C11; eBioscience) and cultured for 4 days. [^{3}H]Thymidine (6.7 Ci/mmol) was added to the culture (1 μCi/well) in the last 16 h. At the end of culture, cells were harvested onto glass fiber filters (Wallac), and the incorporation of [^{3}H]thymidine was measured using scintillation counting. For blocking experiments, anti-TRAIL (clone N2B2) or anti-PD-L1 (clone MIH5) blocking mAb (5 μg/ml) was added to the culture.

Analysis of presentation of MOG epitope by genetically modified ES-DC

MOG epitope-reactive T cells were prepared from inguinal lymph nodes of mice immunized according to protocol for EAE induction described below, using nylon wool columns. X-ray-irradiated (35 Gy) ES-DC as stimulator cells (2×10^4) were cocultured with the MOG-reactive T cells ($1.5–2 \times 10^5$) in wells of 96-well culture plates for 3 days. Proliferation of T cells in

the last 12 h of the culture was quantified based on [^{3}H]thymidine uptake, as described above.

Induction of EAE and treatment with ES-DC

For EAE induction by synthetic peptides or purified protein, 6- to 8-wk-old female CBF_1 mice were immunized by giving a s.c. injection at the base of the tail with a 0.2-ml IFA/PBS solution containing 600 μg of MOG p35–55 peptide and 400 μg of *Mycobacterium tuberculosis* H37Ra (Difco Laboratories) on day 0. In addition, 500 ng of purified *Bordetella pertussis* toxin (Calbiochem) were injected i.p. on days 0 and 2. For EAE induction by ES-DC presenting MOG peptide, ES-DC were injected at the base of the tail of mice (5×10^5 cells/mouse) at day 0, and the mice were given i.p. 500 ng of *B. pertussis* toxin in 0.2 ml of PBS on days 0 and 2. For prevention of EAE, mice were injected i.p. with ES-DC (1×10^6 cells/mouse/injection) on days −8, −5, and −2 (preimmunization treatment), or on days 5, 9, and 13 (postimmunization treatment). The mice were observed over a period of 42 days for clinical signs, and scores were assigned based on the following scale: 0, normal; 1, weakness of the tail and/or paralysis of the distal half of the tail; 2, loss of tail tonicity and abnormal gait; 3, partial hindlimb paralysis; 4, complete hindlimb paralysis; 5, forelimb paralysis or moribundity; 6, death.

Immunohistochemical analysis

Freshly excised spinal cords were immediately frozen and embedded in Tissue-Tek OCT compound (Sakura Finetechnical). Immunohistochemical staining of CD4, CD8, and Mac-1 was done, as described (20), but with some modification. In brief, serial 7-μm sections were made using cryostat and underwent immunochemical staining with mAbs specific to CD4 (clone L3T4; BD Pharmingen), CD8 (clone Ly-2; BD Pharmingen), or Mac-1 (clone M1/70; eBioscience), and N-Histofine Simple Stain Mouse MAX PO (Nichirei). Frozen sections of spleen were subjected to TUNEL staining by using ApopTag Fluorescein In Situ Apoptosis Detection kits (Serologicals). In brief, sections were incubated with digoxigenin-conjugated nucleotides and TdT, and subsequently with peroxidase-conjugated anti-digoxigenin Ab. The staining signals were developed using diaminobenzidene.

Analysis of T cell response to MOG or keyhole limpet hemocyanin (KLH)

Immunization of mice and restimulation of draining lymph node cells in vitro were done as described (26), but with some modification. In brief, ES-DC-treated and control mice were immunized at the base of the tail with MOG peptide, according to protocol for EAE induction, or 50 μg of KLH protein (Sigma-Aldrich) emulsified in CFA. After indicated days, inguinal lymph node cells and spleen cells were isolated and cultured (5×10^5 cells/well) in the presence of MOG peptide (0, 8, 2.5, or 80 μg/ml) or KLH (16, 50, or 160 μg/ml) in 10% horse serum/RPMI 1640/2-ME or 2% mouse serum/DMEM/2-ME/insulin-transferrin-selenium-X (Invitrogen Life Technologies), and the proliferative response was quantified based on [^{3}H]thymidine uptake, as described above. In addition, when mice were immunized with ES-DC expressing MOG peptide for EAE induction, spleen cells were isolated at day 14, and cultured (5×10^5 cells/well) in the presence of MOG peptide in 10% horse serum/RPMI 1640/2-ME, and the proliferative response was quantified based on [^{3}H]thymidine uptake, as described above. To analyze production of cytokines of spleen cells isolated from mice treated with ES-DC, isolated spleen cells were stimulated with 10 μM MOG peptide or irrelevant OVA peptide in vitro. After 72 or 96 h, cell supernatants were harvested and measured for cytokine content using ELISA kits (eBioscience) for IL-4, IL-10, and IFN-γ.

Statistical analysis

Two-tailed Student's *t* test was used to determine the statistical significance of differences. A value of $p < 0.05$ was considered significant.

Results

Induction of EAE in CBF_1 mice

To date, we found no study that EAE had been induced in CBF_1 mice. Therefore, before the study on therapeutic intervention, it was necessary to set up an experimental condition under which we could reproducibly induce EAE in CBF_1 mice. We compared several induction protocols using protein or peptide Ag of MOG, MBP, and PLP. As a result, we found that, when mice were s.c. injected at the base of the tail with a 0.2-ml IFA/PBS solution containing 600 μg of MOG p35–55 and 400 μg of *M. tuberculosis* accompanying an i.p. injection of 500 ng of purified *B. pertussis* toxin on days 0 and 2, EAE is reproducibly induced in CBF_1 mice with an average peak clinical score of 3.3 (Table I). We decided to use this protocol in the following experiments. In addition, inoculation of MBP p35–47, MBP whole protein, or PLP p190–209 together with *M. tuberculosis* and *B. pertussis* toxin also induced EAE in CBF_1 mice with a peak clinical score ranging between 2 and 3 (Table I).

Genetic modification of ES-DC to express MOG peptide along with TRAIL or PD-L1

At the first step in the generation of ES-DC presenting MOG peptide and simultaneously expressing TRAIL or PD-L1, TT2 ES cells were transfected with an expression vector for TRAIL (pCAG-TRAIL-INeo) or PD-L1 (pCAG-PDL1-INeo), as shown in Fig. 1*A*. Then, ES cell clones introduced with either of the expression vectors and parental TT2 ES cells were transfected with the MOG peptide expression vector, pCAG-MOG-IPuro (Fig. 1*B*). In this vector, a cDNA for human Ii was mutated to contain an oligo DNA encoding MOG p35–55 epitope in the CLIP region (1, 2, 27, 28). Resultant single- or double-transfectant ES cell clones were subjected to differentiation to ES-DC. ES-DC expressing MOG peptide, MOG peptide plus TRAIL, and MOG peptide plus PD-L1 were designated as ES-DC-MOG, ES-DC-TRAIL/MOG, and ES-DC-PDL1/MOG, respectively. The expression of mutant human Ii

Table I. *EAE induction in CBF_1 mice*[a]

Expt.	Ag	Ag Dose (μg)	Disease Incidence	Day of Onset	Mean Peak Clinical Score
1	MOG p35–55	200×2^b	1/2	9.0 ± 0	1.5 ± 0
2		400	2/2	11.0 ± 0	4.0 ± 0
3		600	44/44	10.2 ± 1.3	3.3 ± 0.5
4		800	2/2	8.0 ± 0	3.0 ± 0
5	MBP p35–47	200×2^b	0/2		
6		600	8/8	5.5 ± 1.3	3.0 ± 0
7	MBP protein	200×2^b	0/2		
8		600	6/6	9.7 ± 1.8	3.0 ± 0
9	PLP p190–209	200×2^b	0/2		
10		600	2/2	5.0 ± 0	2.0 ± 0

[a] Data are combined from a total of 21 experiments. EAE was induced by S.C. injection at the tail base of a 0.2-ml IFA/PBS solution containing 400 μg of *M. tuberculosis* and indicated peptide or MBP protein once (on day 0) or [b] twice (on days 0 and 7), together with i.p. injections of 500 ng of purified *B. pertussis* toxin on days 0 and 2.

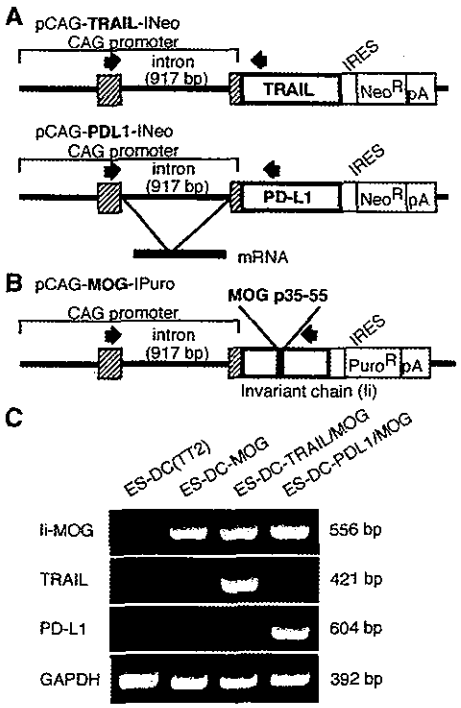

FIGURE 1. Genetic modification of ES-DC to express TRAIL, PD-L1, and Ii-MOG. *A*, The structures of pCAG-TRAIL-INeo and pCAG-PDL1-INeo, the expression vectors for TRAIL and PD-L1, and PCR primers for RT-PCR to detect transgene products are shown. Primer pairs (arrows) were designed to span the intron (917 bp) in the CAG promoter sequence to distinguish PCR products of mRNA origin (421 and 604 bp, respectively) from genome-integrated vector DNA origin. Hatched boxes indicate 5′-untranslated region of the rabbit β-actin gene included in the CAG promoter. The vectors are driven by CAG promoter (pCAG), and cDNA for TRAIL or PD-L1 are followed by the IRES-neomycin-resistance gene (Neo^R)-polyadenylation signal sequence (pA). *B*, The structure of pCAG-MOG-IPuro, the expression vector for mutant human Ii bearing MOG peptide at the CLIP region, are shown as in *A*. Primer pairs (arrows) were designed to generate PCR product of 556 bp originating from transgene-derived mRNA for CAG-MOG. *C*, RT-PCR analysis detected expression of transgene-derived mutant human *Ii* containing the MOG peptide (*Ii-MOG*), *TRAIL*, *PD-L1*, and *GAPDH* (control) mRNA in transfectant ES-DC.

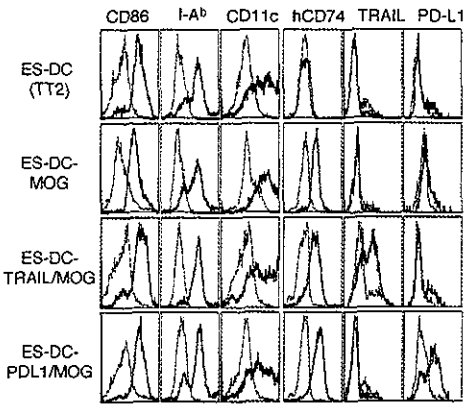

FIGURE 2. Surface phenotype of genetically modified ES-DC. Expression of cell surface CD86, I-A^b, CD11c, TRAIL, and PD-L1 on transfectant ES-DCs was analyzed by flow-cytometric analysis. Expression of mutant human Ii (hCD74) bearing MOG peptide was examined using intracellular staining. Staining patterns with specific Abs (thick line) and isotype-matched control (thin line) are shown.

containing the MOG peptide, TRAIL, and PD-L1 in ES-DC was confirmed by RT-PCR (Fig. 1*C*) and flow-cytometric analysis (Fig. 2). The mutant human Ii containing the MOG peptide was detected by intracellular staining with anti-human CD74 (Ii) mAb (Fig. 2).

ES-DC of similar morphology were generated from any of the transfectant ES cells. As shown in Fig. 2, no significant difference was observed in the level of surface expression of CD86, I-A^b, or CD11c among ES-DC derived from parental TT2 ES cells, ES-DC-MOG, ES-DC-TRAIL/MOG, and ES-DC-PDL1/MOG. Thus, forced expression of TRAIL, PD-L1, or mutant human Ii has little influence on the differentiation of ES-DC.

Functional expression of transgene-derived TRAIL and PD-L1 in ES-DC

The functional activity of TRAIL expressed in ES-DC was analyzed according to the cytotoxicity against TRAIL-sensitive L929 cells. As shown in Fig. 3*A*, ES-DC-TRAIL showed manifest killing activity against L929. In contrast, neither ES-DC (TT2) (parental TT2-derived) nor ES-DC-OVA (OVA-transfected TT2-derived ES-DC) did so. In addition, ES-DC-TRAIL inhibited the proliferation of splenic T cells stimulated with plate-coated anti-CD3 mAb (Fig. 3*B*). PD-L1 expressed on ES-DC also inhibited proliferation of splenic T cells stimulated with anti-CD3 mAb. Inhibition of anti-CD3-induced proliferation of T cells by the TRAIL and PD-L1 was abrogated by addition with anti-TRAIL and anti-PD-L1 blocking mAb, respectively (Fig. 3*B*), but not by isotype-matched control mAb (data not shown). These results indicate that transgene-derived TRAIL and PD-L1 expressed in ES-DC functioned to suppress response of T cells stimulated via TCR/CD3 complexes.

Stimulation of MOG-reactive T cells by ES-DC genetically engineered to express MOG peptide

Presentation of MOG peptide in the context of MHC class II molecules by ES-DC-MOG was investigated in vitro. MOG peptide-reactive T cells were prepared from inguinal lymph nodes of mice, which developed EAE by immunization with MOG p35–55, CFA, and *B. pertussis* toxin. Proliferative response of the MOG-reactive T cells upon coculture with transfectant ES-DC was analyzed. As shown in Fig. 4*A*, ES-DC-MOG stimulated the MOG-reactive T cells to induce proliferation. In contrast, ES-DC carrying Ii-based PCC peptide expression vector (ES-DC-PCC) (2), as a control, did not do so. No proliferative response was observed when naive splenic T cells isolated from syngeneic mice were cocultured with ES-DC-MOG under the same condition (data not shown). These results indicate that the epitope-presenting vector introduced into ES-DC functioned to present the MOG peptide in the context of MHC class II molecules to stimulate MOG-specific $CD4^+$ T cells.

It has been reported that transfer of bone marrow-derived DC preloaded with MOG peptide caused development of EAE in naive mice (29, 30). We presumed that, if ES-DC-MOG could encounter with MOG-specific T cells and stimulate the T cells with MOG peptide in vivo, EAE would be developed. We injected ES-DC-MOG or ES-DC-PCC, as a control, at the base of the tail of naive mice and also gave i.p. 500 ng of *B. pertussis* toxin on the same day and 2 days later. In the results, EAE was developed in the mice transferred with ES-DC-MOG but not those transferred with ES-DC-PCC (Fig. 4*B*).

We examined whether MOG-specific T cells were activated in vivo by injection with ES-DC-MOG. Fourteen days after the injection of ES-DC and *B. pertussis* toxin, spleen cells were isolated

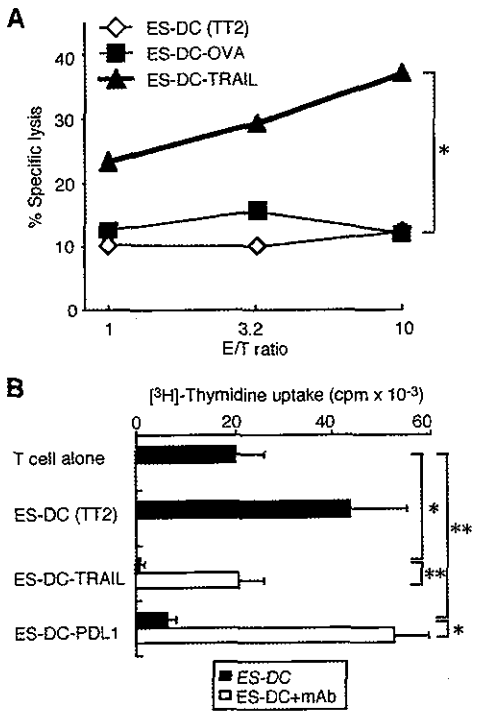

FIGURE 3. Expression of functional TRAIL or PD-L1 in ES-DC transfectants. *A*, The activity of TRAIL expressed in ES-DC was analyzed based on cytotoxicity against L929 cell. ^{51}Cr-labeled target cells (5×10^3 L929 cells) were incubated with ES-DC (TT2), ES-DC-OVA, or ES-DC-TRAIL as effector cells at the indicated E:T ratio for 12 h, and after the incubation, cytolysis of target cells was quantified by measuring radioactivity in the supernatants. Results are expressed as mean specific lysis of triplicate assays, and SDs of triplicates were <4%. *B*, Irradiated ES-DC (TT2), ES-DC-TRAIL, and ES-DC-PDL1 (2×10^4/well) were cocultured with 1×10^5 syngeneic CBF_1 splenic T cells in the presence (□) or absence (■) of blocking Ab (anti-TRAIL mAb or anti-PD-L1 mAb, 5 μg/ml) for 4 days in 96-well flat-bottom culture plates precoated with anti-CD3 mAb. Proliferation of T cells was quantified by measuring [^{3}H]thymidine incorporation. The asterisks indicate that the differences in responses are statistically significant between two values indicated by lines (*, $p < 0.01$; **, $p < 0.05$). The data are each representative of three independent and reproducible experiments with similar results.

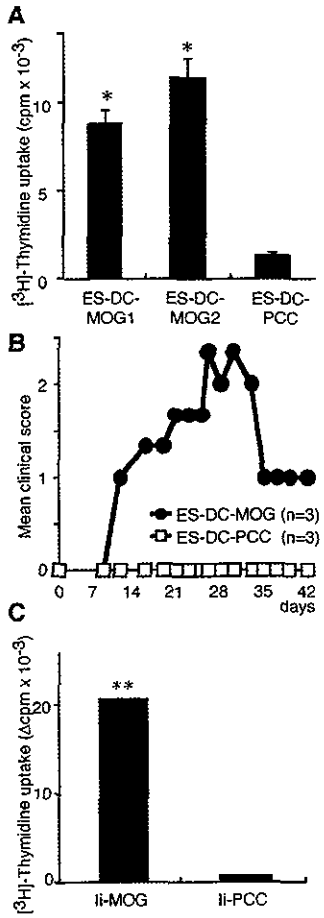

FIGURE 4. Presentation of MOG epitope by ES-DC introduced with Ii-based MOG epitope-presenting vector. *A*, T cells (1.5×10^5) isolated from inguinal lymph nodes of CBF_1 mice immunized according to the protocol for EAE induction were cocultured with one of two independent clones (2×10^4) of ES-DC-MOG or a clone of ES-DC-PCC, presenting PCC epitope, for 3 days. Proliferative response of T cells was quantified by [^{3}H]thymidine uptake in the last 12 h of the culture. *B*, CBF_1 mice (three mice per group) were injected s.c. with ES-DC-MOG or ES-DC-PCC (5×10^5) on day 0, together with i.p. injection of 500 ng of purified *B. pertussis* toxin on days 0 and 2, and the severity of induced EAE was evaluated. The disease incidence, mean day of onset ± SD, and mean peak clinical score ± SD of mice injected with ES-DC-MOG were 100%, 11.3 ± 1.7, and 2.7 ± 0.4, respectively. *C*, Spleen cells were isolated on day 14 from mice treated as in *B*, and whole spleen cells (5×10^5/well) were cultured in the presence of 1 μg/ml MOG peptide for 3 days. Proliferative response was quantified as in *A*. Data were indicated as Δcpm (value in the presence of peptide − value in the absence of peptide ($<46 \times 10^3$ cpm)), and SDs of triplicates were <9% of mean value. The asterisks indicate that the differences in responses are statistically significant compared with ES-DC-PCC (*, $p < 0.01$; **, $p < 0.05$). The data are each representative of three independent and reproducible experiments with similar results.

from the mice and cultured in the presence of MOG peptide. As shown in Fig. 4*C*, the spleen cells isolated from mice injected with ES-DC-MOG showed proliferative response to MOG peptide. In contrast, those isolated from mice injected with ES-DC-PCC did not do so. These results indicate that in vivo transferred ES-DC-MOG together with adjuvant effect of *B. pertussis* toxin stimulated MOG-specific T cells to develop EAE.

Protection from MOG-induced EAE by treatment with ES-DC expressing MOG peptide along with TRAIL or PD-L1

We examined whether TRAIL and PD-L1 expressed by ES-DC together with MOG peptide had an effect to down-modulate MOG-specific T cell responses in vitro. MOG-reactive T cells prepared as described above were cocultured with ES-DC-MOG, ES-DC-TRAIL/MOG, or ES-DC-PDL1/MOG. As shown in Fig. 5, proliferative response of the MOG-reactive T cells cocultured with ES-DC-TRAIL/MOG or ES-DC-PDL1/MOG was significantly lower than those cocultured with ES-DC-MOG, even though the three types of ES-DC expressed an almost equal level of MOG-Ii (Fig. 2). These results indicate down-modulation of the response of MOG-reactive T cells in vitro by TRAIL and PD-L1 coexpressed together with MOG peptide on ES-DC.

We tested whether or not development of EAE would be prevented by pretreatment of mice with genetically modified ES-DC. Mice were i.p. injected with ES-DC-TRAIL/MOG or ES-DC-PDL1/MOG at days −8, −5, and −2 (1×10^6 cells/mouse/injection), and sequentially immunized with MOG peptide plus adjuvants at days 0 and 2 according to the protocol described in Fig. 6*A*. As shown in Fig. 6*B* and Table II, EAE was almost

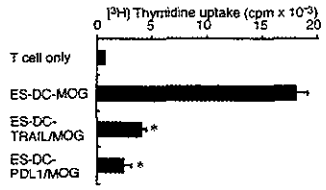

FIGURE 5. Decreased proliferative response to MOG peptide of MOG-reactive T cells cocultured with ES-DC expressing MOG plus TRAIL or MOG plus PD-L1. T cells (2×10^5) isolated from inguinal lymph nodes of CBF_1 mice immunized according to the protocol for EAE induction were cocultured with irradiated ES-DC-MOG, TRAIL/MOG, or PDL1/MOG (2×10^4) for 3 days, as in Fig. 4*A*. The asterisks indicate that the differences in responses are statistically significant ($p < 0.01$) compared with ES-DC-MOG. The data are each representative of three independent and reproducible experiments with similar results.

completely prevented by pretreatment with either of these genetically modified ES-DC. In contrast, pretreatment with ES-DC-MOG, ES-DC-TRAIL/OVA (as irrelevant Ag), or ES-DC-PDL1/OVA had no effect (Fig. 6*C* and Table II). Thus, the prevention depended on both the presentation of the MOG peptide and the expression of TRAIL or PD-L1 by ES-DC. If 2×10^6 of ES-DC-TRAIL/MOG or ES-DC-PDL1/MOG was given as a one-injection administration, EAE was similarly prevented (data not shown). However, if 5×10^5 of ES-DC-TRAIL/MOG or ES-DC-PDL1/MOG was used for one injection, the disease severity was not reduced (data not shown). Thus, $\sim 1 \times 10^6$ of genetically modified ES-DC as one-injection dose is apparently necessary for the prevention of EAE under this experimental condition.

We asked whether TRAIL or PD-L1 should be coexpressed by the same ES-DC as one presenting MOG peptide for their capacity to protect mice from EAE. As shown in Fig. 6*D* and Table II, coinjection of ES-DC-MOG together with ES-DC-TRAIL or ES-DC-PDL1 did not reduce the severity of EAE. Thus, coexpression of TRAIL or PD-L1 with MOG peptide by ES-DC is necessary for the protection from EAE. These results emphasize the advantage of the technology of ES cell-mediated genetic modification of DC, by which one can generate clonal transfectant DC carrying multiple expression vectors.

Next, we tested whether or not treatment with ES-DC after immunization with MOG would achieve some preventive effect on EAE. As shown in Fig. 7*A*, mice were immunized according to the protocol for EAE induction and, after that, injected with ES-DC on days 5, 9, and 13 (1×10^6 cells/mouse/injection). Even in this postimmunization treatment, injection of ES-DC-TRAIL/MOG or ES-DC-PDL1/MOG reduced severity of the disease, but ES-DC-MOG did not do so (Fig. 7*B* and Table II).

Decreased T cell response to MOG in mice treated with ES-DC-TRAIL/MOG or -PD-L1/MOG

We examined whether treatment with ES-DC-TRAIL/MOG or -PDL1/MOG would reduce the activation of MOG-specific T cells. Forty-two days after the immunization according to the protocol for EAE induction (Fig. 6*A*), we isolated inguinal lymph node cells and analyzed their proliferative response upon restimulation in vitro with MOG peptide. As shown in Fig. 8*A*, the magnitude of proliferation of lymph node cells isolated from mice treated with ES-DC-TRAIL/MOG or -PDL1/MOG was not increased in response to MOG peptide. In contrast, that of lymph node cells from ES-DC-MOG-treated or untreated mice was increased with statistical significance. In the presence of 25 μg/ml MOG peptide, stimulation index (count in the presence of MOG peptide/count in the absence of Ag) for that of untreated, ES-DC-MOG, -TRAIL/MOG, and -PDL1/MOG-treated mice were 2.8, 2.4, 1.3, and 1.0, respectively. These results suggest that treatment with ES-DC-TRAIL/MOG or -PDL1/MOG inhibited the activation of MOG-specific T cells or reduced their number in mice immunized with MOG peptide and adjuvants.

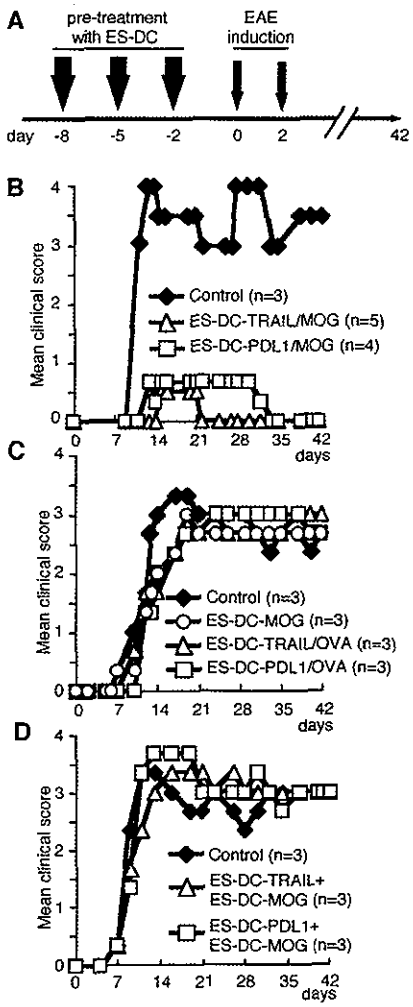

FIGURE 6. Prevention of MOG-induced EAE by pretreatment of mice with ES-DC expressing MOG plus TRAIL or MOG plus PD-L1. *A*, The schedule for pretreatment and induction of EAE is shown. CBF_1 mice (three to five mice per group) were i.p. injected with ES-DC (1×10^6 cells/injection/mouse) on days −8, −5, and −2. EAE was induced by s.c. injection of MOG peptide plus *M. tuberculosis* H37Ra emulsified in IFA on day 0, and i.p. injection of *B. pertussis* toxin on days 0 and 2. *B–D*, Disease severity of mice treated with ES-DC-TRAIL/MOG, ES-DC-PDL1/MOG, or RPMI 1640 medium (control) (*B*), ES-DC-MOG, ES-DC-TRAIL/OVA, ES-DC-PDL1/OVA, or RPMI 1640 medium (control) (*C*), coinjection with ES-DC-MOG plus ES-DC-TRAIL, ES-DC-MOG plus ES-DC-PDL1, or RPMI 1640 medium (control) (*D*) is shown. The data are each representative of at least two independent and reproducible experiments, and data of all experiments are summarized in Table II.

Next, we examined whether or not treatment with ES-DC would affect immune responses to an irrelevant exogenous Ag. We treated mice with ES-DC-MOG, -TRAIL/MOG, -PDL1/MOG, or RPMI 1640 medium (control) using the same schedule described above, and subsequently immunized the mice with KLH/CFA. Eleven days after the immunization, we isolated inguinal lymph

Table II. *Suppression of EAE induction in CBF$_1$ mice treated with ES-DC*[a]

Treatment (ES-DC)	Disease Incidence	Day of Onset	Mean Peak Clinical Score
No Treatment (control)	26/26	10.5 ± 1.1	3.3 ± 0.4
Pre[b]- TRAIL/MOG	**3/10**	18.3 ± 2.4	**0.3 ± 0.4**
Pre- PDL1/MOG	**5/10**	13.4 ± 2.1	**0.8 ± 0.8**
Pre- MOG	8/8	10.5 ± 1.3	3.0 ± 0.3
Pre- TRAIL/OVA	6/6	10.2 ± 2.9	3.0 ± 0
Pre- PDL1/OVA	6/6	11.3 ± 0.9	3.0 ± 0
Pre- TRAIL + MOG	6/6	10.2 ± 1.2	3.2 ± 0.6
Pre- PDL1 + MOG	6/6	10.2 ± 0.6	3.3 ± 0.7
Post[c]- TRAIL/MOG	**3/6**	18.7 ± 4.4	**0.5 ± 0.5**
Post- PDL1/MOG	**3/6**	13.7 ± 1.1	**1.0 ± 1.0**
Post- MOG	6/6	10.8 ± 1.0	3.2 ± 0.3

[a] Data are combined from a total of 10 separate experiments including those shown in Figs. 6 and 7. EAE was induced by s.c. injection at the tail base of a 0.2-ml IFA/PBS solution containing 400 μg of *M. tuberculosis* and 600 μg of MOG peptide once (on day 0), together with i.p. injections of 500 ng of purified *B. pertussis* toxin *on days 0 and 2*. For prevention of EAE, mice were injected i.p. with ES-DC (1×10^6 cells/mouse/injection) [b]on days −8, −5, and −2 (preimmunization treatment), or [c]on days 5, 9, and 13 (postimmunization treatment). The incidence and the clinical score reduced by ES-DC treatment are indicated in boldface.

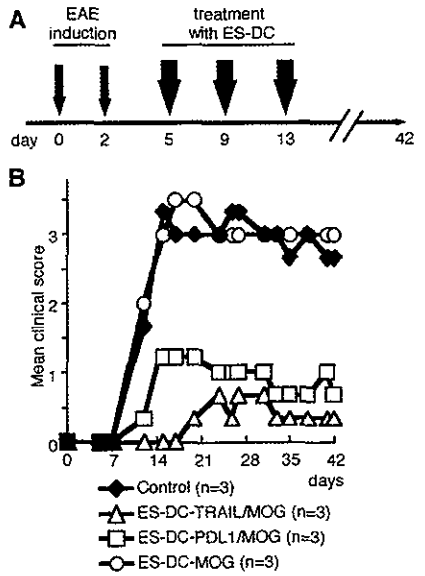

FIGURE 7. Inhibition of MOG-induced EAE by treatment with ES-DC expressing MOG plus TRAIL or MOG plus PD-L1 after immunization with MOG. *A*, The schedule for induction of EAE and treatment is shown. CBF$_1$ mice (three mice per group) were immunized on days 0 and 2 according to the EAE induction schedule described above, and subsequently i.p. injected with ES-DC (1×10^6 cells/injection/mouse) on days 5, 9, and 13. *B*, Disease severity of mice treated with ES-DC-TRAIL/MOG, ES-DC-PD-L1/MOG, ES-DC-MOG, or RPMI 1640 medium (control) is shown. The data are each representative of two independent and reproducible experiments, and data of all experiments are summarized in Table II.

node cells and analyzed their proliferative response upon restimulation with KLH in vitro. As a result, lymph node cells of ES-DC-treated and control mice showed the same magnitude of proliferative response (Fig. 8*B*), thereby indicating that the treatment with such genetically modified ES-DC did not affect the immune response to irrelevant Ags.

We immunohistochemically analyzed spinal cord, the target organ of the disease, of mice subjected to EAE induction with or without treatment with ES-DC. Massive infiltration of CD4$^+$ T cells, CD8$^+$ T cells, and Mac-1$^+$ macrophages was observed in spinal cords of untreated control mice (Fig. 9). In contrast, T cells and macrophages hardly infiltrated into the spinal cord of mice treated with ES-DC-TRAIL/MOG or ES-DC-PDL1/MOG. The results of histological analysis are in parallel with the severity of EAE and activation state of MOG-specific T cells of each mouse.

Increased number of apoptotic cells in splenic CD4$^+$ T cells by treatment with ES-DC-TRAIL/MOG

With regard to the mechanism of prevention of EAE by transfectant ES-DC, we analyzed the apoptosis of CD4$^+$ T cell in spleens of mice treated with ES-DC by staining with annexin V and subsequent flow-cytometric analysis. In the results, we observed that transfer of ES-DC-TRAIL/MOG caused an increase of apoptosis of CD4$^+$ T cells in recipient mice (17.3 ± 2.5%), compared with transfer of ES-DC-MOG (12.0 ± 0.4%), ES-DC-PDL1/MOG (12.2 ± 0.5%), or RPMI 1640 medium control (10.2 ± 0.8%). In the experiments, three mice were used for each group. Increased numbers of apoptotic cells in spleen of mice transferred with ES-DC-TRAIL/MOG were also observed in histological analysis with TUNEL staining (Fig. 10). The capacity of ES-DC-TRAIL/MOG to cause apoptosis of T cells may play some role in the protection from EAE.

Discussion

DC are the most potent APC responsible for priming of naive T cells in initiation of the immune response. Recent studies revealed that DC are also involved in the maintenance of immunological self-tolerance, promoting T cells with regulatory functions, or inducing anergy of T cells. In vivo transfer of Ag-loaded DC with a tolerogenic character is regarded as a promising therapeutic means to negatively manipulate immune response in an Ag-specific manner. Various culture procedures used to generate DC with a tolerogenic character have been reported (31–36). Mouse bone marrow-derived DC generated in the presence of IL-10 and/or TGF-β or in the low dose of GM-CSF showed immature phenotypes, a low-level expression of cell surface MHC and costimulatory molecules, and induced T cell anergy in vitro and tolerance to specific Ags or allogeneic transplanted organs in vivo. In humans, monocyte-derived immature DC loaded with antigenic peptides and transferred in vivo have been shown to cause the Ag-specific immune suppression (37).

Genetic modification may be a more steady and reliable way to manipulate the character of DC. Generation of tolerogenic DC by forced expression of Fas ligand, indoleamine 2,3-dioxygemase, IL-10, or CTLA4Ig by gene transfer has been also reported (38–41). In a recent study, type II collagen-loaded bone marrow-derived DC genetically engineered to express TRAIL by using an adenovirus vector ameliorated type II collagen-induced arthritis (42).

Regarding methods for gene transfer to DC, electroporation, lipofection, and virus vector-mediated transfection have been reported (38–43). However, considering clinical applications, presently established methods have several drawbacks, i.e., efficiency of gene transfer, stability of gene expression, limitation of the size and number of genes to be introduced, potential risk accompanying the use of virus vectors, and the immunogenicity of the virus vectors. For the purpose of Ag-specific negative regulation of immune responses, the antigenicity of vector systems may lead to problems. Importantly, to efficiently down-modulate T cell responses in an Ag-specific manner, it is desirable to introduce multiple expression vectors to generate stable transfectant DC, which continuously present transgene-derived Ag and simultaneously express immunosuppressive molecules.

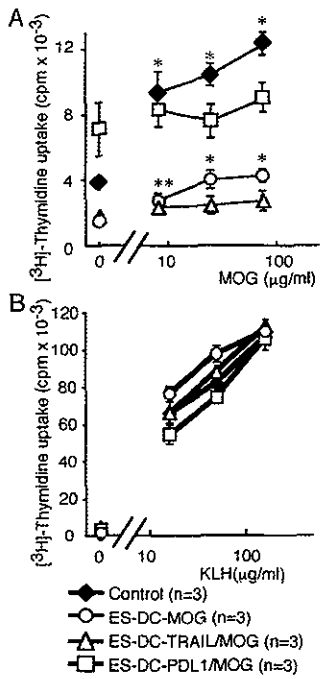

FIGURE 8. Inhibition of activation of MOG-reactive T cells and no effect of activation of KLH-specific T cell by treatment of mice with ES-DC expressing MOG plus TRAIL or PD-L1. *A*, Inguinal lymph node cells (3×10^5) were isolated from CBF_1 mice (three mice per group) of various treatment groups at over day 42, and were stimulated ex vivo with irradiated and MOG peptide-pulsed syngeneic spleen cells for 3 days. Proliferative response of T cells was quantified by [^{3}H]thymidine uptake in the last 12 h of the culture. The asterisks indicate that the differences in responses are statistically significant compared with count in the absence of Ag (*, $p < 0.01$; **, $p < 0.05$). The data are each representative of two independent and reproducible experiments with similar results. *B*, CBF_1 mice (three mice per group) were i.p. injected with ES-DC (1×10^6 cells/injection/mouse) on days −8, −5, and −2, and immunized with KLH/CFA on day 0. On day 11, inguinal lymph node cells were isolated and restimulated with the indicated concentration of KLH in vitro. Proliferation of T cells was quantified as described above.

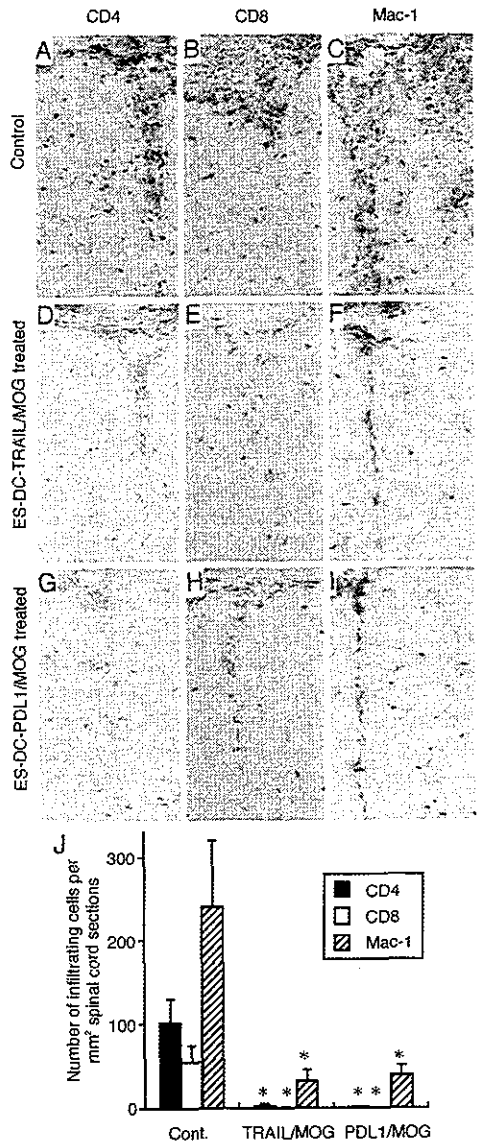

FIGURE 9. Inhibition of infiltration of $CD4^+$ T cells, $CD8^+$ T cells, and Mac-1^+ macrophages into spinal cord by treatment of mice with ES-DC expressing MOG plus TRAIL or PD-L1. Mice were pretreated with ES-DC-TRAIL/MOG, PDL1/MOG, or untreated and subsequently immunized according to the protocol for EAE induction as shown in Fig. 6*A*. The cervical, thoracic, and lumbar spinal cord was isolated at day 11 and subjected to immunohistochemical analysis. CD4 (*A*, *D*, and *G*), CD8 (*B*, *E*, and *H*), and Mac-1 (*C*, *F*, and *I*) staining are shown in representative untreated control (*A–C*), ES-DC-TRAIL/MOG-treated (*D–F*), and ES-DC-PDL1/MOG-treated (*G–J*) mice. *J*, The positive cells were microscopically counted in three sections of spinal cord. Results are expressed as mean ± SD of $CD4^+$, $CD8^+$, Mac-1^+ cells per 1 mm^2 tissue area of samples obtained from five mice. The asterisks indicate that the decreases in number of infiltrated cells are statistically significant ($p < 0.01$) compared with control.

Efficient genetic modification of mouse DC can be done by gene transfer to ES cells and subsequent differentiation of transfectant ES cells to ES-DC. By sequential transfection of ES cells using multiple expression vectors, transfectant ES-DC expressing multiple transgene products can readily be generated. In a recent study, we demonstrated that this methodology worked very effectively for induction of antitumor immunity, showing highly efficient stimulation of Ag-specific T cells by in vivo transfer of ES-DC expressing T cell-attracting chemokines along with Ag (20).

The present study demonstrates the usefulness of the genetically modified DC generated by this method for the treatment of subjects with autoimmune disease. We generated ES-DC presenting the MOG epitope in the context of MHC class II molecule and simultaneously expressing immunosuppressive molecule, TRAIL or PD-L1. By pre- or posttreatment of mice with such ES-DC, we succeeded in preventing an autoimmune disease model, EAE induced by immunization with MOG peptide (Figs. 6 and 7; Table II). Down-modulation of immune response by treatment with genetically modified ES-DC did not affect the immune response to irrelevant exogenous Ag, KLH (Fig. 8*B*). Thus, we achieved the prevention of EAE without decrease in the immune response to an irrelevant Ag.

As for the function of TRAIL, induction of apoptosis has been reported by several groups (3, 4, 42, 44). We also observed an increase in apoptosis of $CD4^+$ T cells in spleens of mice treated with ES-DC-TRAIL/MOG compared with ES-DC-MOG, PDL1/MOG or RPMI 1640 medium (control), as shown in Fig. 10. The result is consistent with a recent report by Liu et al. (42). They introduced the *TRAIL* gene into bone marrow-derived DC by adenovirus vector and injected the *TRAIL* transfectant DC into mice for prevention of collagen-induced arthritis, and also observed an increased number of apoptotic T cells in the injected mice. The

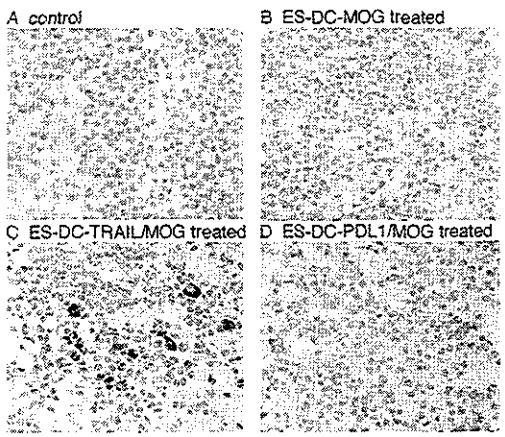

FIGURE 10. Induction of apoptosis of spleen cells by treatment of mice with ES-DC expressing TRAIL along with MOG peptide. Mice were treated with the indicated ES-DC and immunized with MOG peptide, following the schedule described in Fig. 6*A*. On day 11, spleens were isolated from the mice, and apoptotic cells were detected by in situ TUNEL staining. Original magnification, ×200. Sections of the mice untreated (*A*), treated with ES-DC-MOG (*B*), ES-DC-TRAIL/MOG (*C*), and ES-DC-PDL1/MOG (*D*) are shown. Similar results were observed for three mice used in each experimental group, and representative results are shown.

potential for ES-DC-TRAIL/MOG to cause apoptosis of T cells may have played some role in the protection from EAE, at least in part, in our experiments. In addition, our preliminary experiments suggest that ES-DC-TRAIL/MOG induced T cells with protective effects against EAE. In the experiments, we isolated splenic $CD4^+$ T cells from ES-DC-TRAIL/MOG-treated mice and adoptively transferred them to naive mice. The severity of subsequently induced EAE in the recipient mice was significantly reduced by this treatment (data not shown). At present, it may be possible that both induction of apoptosis of MOG-reactive pathogenic T cells and promotion of T cells with some regulatory function contributed to prevention of EAE by ES-DC-TRAIL/MOG. However, to clarify the precise mechanism or character of the T cell with regulatory function, further investigations are necessary.

In contrast, in case of treatment with ES-DC-PDL1/MOG, neither apoptosis of T cells nor induction of transferable disease-preventing T cells was observed (data not shown). We presume induction of anergy of MOG-reactive T cells to be likely as the mechanism of disease-preventive effect of treatment with ES-DC-PDL1/MOG, based on previous literature regarding the function of PD-L1 (7, 14, 45–47).

To determine whether the profile of cytokine production was altered by treatment with ES-DC, we did ELISA to quantify IL-10, IL-4, and IFN-γ produced by spleen cells of ES-DC-treated mice upon stimulation with MOG peptide in vitro. We observed no significant change in the amount of these cytokines produced by spleen cells from ES-DC-TRAIL/MOG-treated or ES-DC-PDL1/MOG-treated mice, compared with those from ES-DC-MOG-treated mice (data not shown). The level of expression of mRNA for TGF-β detected by RT-PCR was also unchanged compared with control (data not shown). Thus, involvement of IL-10-producing Tr-1 cells or Th2 cells in protection from EAE by treatment with ES-DC-TRAIL/MOG or ES-DC-PDL1/MOG is unlikely, although one cannot totally rule out the possibility.

The capacity of the ES cells to differentiate to ES-DC was never impaired even after culture for at least over 4 mo. Inactivation of transcription of introduced genes due to gene silencing in ES cells can be prevented using vectors bearing the IRES-drug resistance gene or by targeted gene introduction with an exchangeable gene-trap system (2). Thus, genetically manipulated ES cells can be used as an infinite source for DC with genetically modified properties.

Recently, we established methods for generation of DC from nonhuman primate ES cells and also for genetic modification of them (S. Senju, H. Suemori, H. Matsuyoshi, S. Hirata, Y. Uemura, Y.-Z. Chen, D. Fukuma, M. Furuya, N. Nakatsuji, and Y. Nishimura, manuscript in preparation). We hope to apply this method to human ES cells to generate genetically modified human ES-DC, although some modification might be necessary. In the future, Ag-specific immune modulation therapy by in vivo transfer of human ES-DC expressing antigenic protein along with immune-regulating molecules may well be realized, based on evidence in the current study in the mouse system. Possible applications of this technology are treatment of subjects with autoimmune and allergic diseases and also for induction of tolerance to transplanted organs, especially those generated from ES cells. Thus, the methods established in the present study may have implications as a broad medical technology.

Acknowledgments

We thank Dr. S. Aizawa (RIKEN Center for Developmental Biology, Kobe, Japan) for TT2, Drs. N. Takakura (Kanazawa University, Kanazawa, Japan) and T. Suda (Keio University, Tokyo, Japan) for OP9, Dr. H. Niwa (RIKEN Center for Developmental Biology, Kobe, Japan) for pCAG-IPuro, Drs. T. Okazaki and T. Honjo (Kyoto University, Kyoto, Japan) for a cDNA clone for PD-L1, Tatsuko Kubo (Department of Molecular Pathology, Kumamoto University) for technical assistance, and Kirin Brewery Co., Ltd., for rGM-CSF. M. Ohara (Fukuoka, Japan) provided helpful comments on the manuscript.

References

1. Fujii, S., S. Senju, Y. Z. Chen, M. Ando, S. Matsushita, and Y. Nishimura. 1998. The CLIP-substituted invariant chain efficiently targets an antigenic peptide to HLA class II pathway in L cells. *Hum. Immunol. 59:607.*
2. Senju, S., S. Hirata, H. Matsuyoshi, M. Masuda, Y. Uemura, K. Araki, K. Yamamura, and Y. Nishimura. 2003. Generation and genetic modification of dendritic cells derived from mouse embryonic stem cells. *Blood 101:3501.*
3. Wiley, S. R., K. Schooley, P. J. Smolak, W. S. Din, C. P. Huang, J. K. Nicholl, G. R. Sutherland, T. D. Smith, C. Rauch, C. A. Smith, and R. G. Goodwin. 1995. Identification and characterization of a new member of the TNF family that induces apoptosis. *Immunity 3:673.*
4. Kayagaki, N., N. Yamaguchi, M. Nakayama, K. Takeda, H. Akiba, H. Tsutsui, H. Okamura, K. Nakanishi, K. Okumura, and H. Yagita. 1999. Expression and function of TNF-related apoptosis-inducing ligand on murine activated NK cells. *J. Immunol. 163:1906.*
5. Lamhamedi-Cherradi, S. E., S. J. Zheng, K. A. Maguschak, J. Peschon, and Y. H. Chen. 2003. Defective thymocyte apoptosis and accelerated autoimmune diseases in $TRAIL^{-/-}$ mice. *Nat. Immunol. 4:255.*
6. Dong, H., G. Zhu, K. Tamada, and L. Chen. 1999. B7-H1, a third member of the B7 family, co-stimulates T-cell proliferation and interleukin-10 secretion. *Nat. Med. 5:1365.*
7. Freeman, G. J., A. J. Long, Y. Iwai, K. Bourque, T. Chernova, H. Nishimura, L. J. Fitz, N. Malenkovich, T. Okazaki, M. C. Byrne, et al. 2000. Engagement of the PD-1 immunoinhibitory receptor by a novel B7 family member leads to negative regulation of lymphocyte activation. *J. Exp. Med. 192:1027.*
8. Nishimura, H., M. Nose, H. Hiai, N. Minato, and T. Honjo. 1999. Development of lupus-like autoimmune diseases by disruption of the *PD-1* gene encoding an ITIM motif-carrying immunoreceptor. *Immunity 11:141.*
9. Nishimura, H., T. Okazaki, Y. Tanaka, K. Nakatani, M. Hara, A. Matsumori, S. Sasayama, A. Mizoguchi, H. Hiai, N. Minato, and T. Honjo. 2001. Autoimmune dilated cardiomyopathy in PD-1 receptor-deficient mice. *Science 291:319.*
10. Song, K., Y. Chen, R. Goke, A. Wilmen, C. Seidel, A. Goke, and B. Hilliard. 2000. Tumor necrosis factor-related apoptosis-inducing ligand (TRAIL) is an inhibitor of autoimmune inflammation and cell cycle progression. *J. Exp. Med. 191:1095.*
11. Hilliard, B., A. Wilmen, C. Seidel, T. S. Liu, R. Goke, and Y. Chen. 2001. Roles of TNF-related apoptosis-inducing ligand in experimental autoimmune encephalomyelitis. *J. Immunol. 166:1314.*
12. Lunemann, J. D., S. Waiczies, S. Ehrlich, U. Wendling, B. Seeger, T. Kamradt, and F. Zipp. 2002. Death ligand TRAIL induces no apoptosis but inhibits activation of human (auto)antigen-specific T cells. *J. Immunol. 168:4881.*
13. Kayagaki, N., N. Yamaguchi, M. Abe, S. Hirose, T. Shirai, K. Okumura, and H. Yagita. 2002. Suppression of antibody production by TNF-related apoptosis-inducing ligand (TRAIL). *Cell. Immunol. 219:82.*

14. Nishimura, H., and T. Honjo. 2001. PD-1: an inhibitory immunoreceptor involved in peripheral tolerance. *Trends Immunol. 22:265.*
15. Okazaki, T., Y. Iwai, and T. Honjo. 2002. New regulatory co-receptors: inducible co-stimulator and PD-1. *Curr. Opin. Immunol. 14:779.*
16. Salama, A. D., T. Chitnis, J. Imitola, M. J. Ansari, H. Akiba, F. Tushima, M. Azuma, H. Yagita, M. H. Sayegh, and S. J. Khoury. 2003. Critical role of the programmed death-1 (PD-1) pathway in regulation of experimental autoimmune encephalomyelitis. *J. Exp. Med. 198:71.*
17. Liang, S. C., Y. E. Latchman, J. E. Buhlmann, M. F. Tomczak, B. H. Horwitz, G. J. Freeman, and A. H. Sharpe. 2003. Regulation of PD-1, PD-L1, and PD-L2 expression during normal and autoimmune responses. *Eur. J. Immunol. 33:2706.*
18. Ansari, M. J., A. D. Salama, T. Chitnis, R. N. Smith, H. Yagita, H. Akiba, T. Yamazaki, M. Azuma, H. Iwai, S. J. Khoury, et al. 2003. The programmed death-1 (PD-1) pathway regulates autoimmune diabetes in nonobese diabetic (NOD) mice. *J. Exp. Med. 198:63.*
19. Fairchild, P. J., F. A. Brook, R. L. Gardner, L. Graca, V. Strong, Y. Tone, M. Tone, K. F. Nolan, and H. Waldmann. 2000. Directed differentiation of dendritic cells from mouse embryonic stem cells. *Curr. Biol. 10:1515.*
20. Matsuyoshi, H., S. Senju, S. Hirata, Y. Yoshitake, Y. Uemura, and Y. Nishimura. 2004. Enhanced priming of antigen-specific CTLs in vivo by embryonic stem cell-derived dendritic cells expressing chemokine along with antigenic protein: application to antitumor vaccination. *J. Immunol. 172:776.*
21. Fairchild, P. J., K. F. Nolan, S. Cartland, L. Graca, and H. Waldmann. 2003. Stable lines of genetically modified dendritic cells from mouse embryonic stem cells. *Transplantation 76:606.*
22. Cheng, P., Y. Nefedova, L. Miele, B. A. Osborne, and D. Gabrilovich. 2003. Notch signaling is necessary but not sufficient for differentiation of dendritic cells. *Blood 102:3980.*
23. Mendel, I., N. Kerlero de Rosbo, and A. Ben-Nun. 1995. A myelin oligodendrocyte glycoprotein peptide induces typical chronic experimental autoimmune encephalomyelitis in H-2^b mice: fine specificity and T cell receptor Vβ expression of encephalitogenic T cells. *Eur. J. Immunol. 25:1951.*
24. Greer, J. M., R. A. Sobel, A. Sette, S. Southwood, M. B. Lees, and V. K. Kuchroo. 1996. Immunogenic and encephalitogenic epitope clusters of myelin proteolipid protein. *J. Immunol. 156:371.*
25. Zamvil, S. S., D. J. Mitchell, M. B. Powell, K. Sakai, J. B. Rothbard, and L. Steinman. 1988. Multiple discrete encephalitogenic epitopes of the autoantigen myelin basic protein include a determinant for I-E class II-restricted T cells. *J. Exp. Med. 168:1181.*
26. Senju, S., K. Iyama, H. Kudo, S. Aizawa, and Y. Nishimura. 2000. Immunocytochemical analyses and targeted gene disruption of GTPBP1. *Mol. Cell. Biol. 20:6195.*
27. Fujii, S., Y. Uemura, L. K. Iwai, M. Ando, S. Senju, and Y. Nishimura. 2001. Establishment of an expression cloning system for $CD4^+$ T cell epitopes. *Biochem. Biophys. Res. Commun. 284:1140.*
28. Uemura, Y., S. Senju, K. Maenaka, L. K. Iwai, S. Fujii, H. Tabata, H. Tsukamoto, S. Hirata, Y. Z. Chen, and Y. Nishimura. 2003. Systematic analysis of the combinatorial nature of epitopes recognized by TCR leads to identification of mimicry epitopes for glutamic acid decarboxylase 65-specific TCRs. *J. Immunol. 170:947.*
29. Weir, C. R., K. Nicolson, and B. T. Backstrom. 2002. Experimental autoimmune encephalomyelitis induction in naive mice by dendritic cells presenting a self-peptide. *Immunol. Cell Biol. 80:14.*
30. Legge, K. L., R. K. Gregg, R. Maldonado-Lopez, L. Li, J. C. Caprio, M. Moser, and H. Zaghouani. 2002. On the role of dendritic cells in peripheral T cell tolerance and modulation of autoimmunity. *J. Exp. Med. 196:217.*
31. Bonham, C. A., L. Lu, R. A. Banas, P. Fontes, A. S. Rao, T. E. Starzl, A. Zeevi, and A. W. Thomson. 1996. TGF-β1 pretreatment impairs the allostimulatory function of human bone marrow-derived antigen-presenting cells for both naive and primed T cells. *Transpl. Immunol. 4:186.*
32. Lutz, M. B., R. M. Suri, M. Niimi, A. L. Ogilvie, N. A. Kukutsch, S. Rossner, G. Schuler, and J. M. Austyn. 2000. Immature dendritic cells generated with low doses of GM-CSF in the absence of IL-4 are maturation resistant and prolong allograft survival in vivo. *Eur. J. Immunol. 30:1813.*
33. Steinbrink, K., M. Wolfl, H. Jonuleit, J. Knop, and A. H. Enk. 1997. Induction of tolerance by IL-10-treated dendritic cells. *J. Immunol. 159:4772.*
34. Menges, M., S. Rossner, C. Voigtlander, H. Schindler, N. A. Kukutsch, C. Bogdan, K. Erb, G. Schuler, and M. B. Lutz. 2002. Repetitive injections of dendritic cells matured with tumor necrosis factor-α induce antigen-specific protection of mice from autoimmunity. *J. Exp. Med. 195:15.*
35. Sato, K., N. Yamashita, M. Baba, and T. Matsuyama. 2003. Regulatory dendritic cells protect mice from murine acute graft-versus-host disease and leukemia relapse. *Immunity 18:367.*
36. Sato, K., N. Yamashita, M. Baba, and T. Matsuyama. 2003. Modified myeloid dendritic cells act as regulatory dendritic cells to induce anergic and regulatory T cells. *Blood 101:3581.*
37. Dhodapkar, M. V., R. M. Steinman, J. Krasovsky, C. Munz, and N. Bhardwaj. 2001. Antigen-specific inhibition of effector T cell function in humans after injection of immature dendritic cells. *J. Exp. Med. 193:233.*
38. Takayama, T., Y. Nishioka, L. Lu, M. T. Lotze, H. Tahara, and A. W. Thomson. 1998. Retroviral delivery of viral interleukin-10 into myeloid dendritic cells markedly inhibits their allostimulatory activity and promotes the induction of T-cell hyporesponsiveness. *Transplantation 66:1567.*
39. Lu, L., A. Gambotto, W. C. Lee, S. Qian, C. A. Bonham, P. D. Robbins, and A. W. Thomson. 1999. Adenoviral delivery of CTLA4Ig into myeloid dendritic cells promotes their in vitro tolerogenicity and survival in allogeneic recipients. *Gene Ther. 6:554.*
40. Min, W. P., R. Gorczynski, X. Y. Huang, M. Kushida, P. Kim, M. Obataki, J. Lei, R. M. Suri, and M. S. Cattral. 2000. Dendritic cells genetically engineered to express Fas ligand induce donor-specific hyporesponsiveness and prolong allograft survival. *J. Immunol. 164:161.*
41. Terness, P., T. M. Bauer, L. Rose, C. Dufter, A. Watzlik, H. Simon, and G. Opelz. 2002. Inhibition of allogeneic T cell proliferation by indoleamine 2,3-dioxygenase-expressing dendritic cells: mediation of suppression by tryptophan metabolites. *J. Exp. Med. 196:447.*
42. Liu, Z., X. Xu, H. C. Hsu, A. Tousson, P. A. Yang, Q. Wu, C. Liu, S. Yu, H. G. Zhang, and J. D. Mountz. 2003. CII-DC-AdTRAIL cell gene therapy inhibits infiltration of CII-reactive T cells and CII-induced arthritis. *J. Clin. Invest. 112:1332.*
43. Morita, Y., J. Yang, R. Gupta, K. Shimizu, E. A. Shelden, J. Endres, J. J. Mule, K. T. McDonagh, and D. A. Fox. 2001. Dendritic cells genetically engineered to express IL-4 inhibit murine collagen-induced arthritis. *J. Clin. Invest. 107:1275.*
44. Giovarelli, M., P. Musiani, G. Garotta, R. Ebner, E. Di Carlo, Y. Kim, P. Cappello, L. Rigamonti, P. Bernabei, F. Novelli, et al. 1999. A "stealth effect": adenocarcinoma cells engineered to express TRAIL elude tumor-specific and allogeneic T cell reactions. *J. Immunol. 163:4886.*
45. Brown, J. A., D. M. Dorfman, F. R. Ma, E. L. Sullivan, O. Munoz, C. R. Wood, E. A. Greenfield, and G. J. Freeman. 2003. Blockade of programmed death-1 ligands on dendritic cells enhances T cell activation and cytokine production. *J. Immunol. 170:1257.*
46. Carter, L., L. A. Fouser, J. Jussif, L. Fitz, B. Deng, C. R. Wood, M. Collins, T. Honjo, G. J. Freeman, and B. M. Carreno. 2002. PD-1:PD-L inhibitory pathway affects both $CD4^+$ and $CD8^+$ T cells and is overcome by IL-2. *Eur. J. Immunol. 32:634.*
47. Selenko-Gebauer, N., O. Majdic, A. Szekeres, G. Hofler, E. Guthann, U. Korthauer, G. Zlabinger, P. Steinberger, W. F. Pickl, H. Stockinger, et al. 2003. B7-H1 (programmed death-1 ligand) on dendritic cells is involved in the induction and maintenance of T cell anergy. *J. Immunol. 170:3637.*

Parasitology Research
© Springer-Verlag 2005
DOI 10.1007/s00436-004-1296-0

Original Paper

Expression of TGF-β-like molecules in the life cycle of *Schistosoma japonicum*

M. Hirata (✉) · K. Hirata · T. Hara · M. Kawabuchi · T. Fukuma

M. Hirata · T. Hara · T. Fukuma
Department of Parasitology, Kurume University School of Medicine, 830-0011 Kurume, Japan

K. Hirata · M. Kawabuchi
Department of Anatomy and Cell Biology, Graduate School of Medical Sciences, Kyushu University, 812-8582 Fukuoka , Japan

✉ M. Hirata
Phone: +81-942-317550
Fax: +81-942-310344
E-mail: hiramizu@med.kurume-u.ac.jp

Received: 19 November 2004 / **Accepted:** 23 November 2004

Abstract The transforming growth factor β (TGF-β) family controls an extremely wide range of biological activities, such as the growth and differentiation of cells, and immunological events against infectious agents. Although TGF-β homologs appear to be widely present in metazoan animals, studies of parasite-derived molecules are relatively few. Using antibodies against anti-mouse TGF-β_1, -β_2, and -β_3, we show the expression of TGF-β-like molecules in *Schistosoma japonicum* cercariae, schistosomula, eggs and adult worms. Intense immunoreactivity was found on the surface of free-living cercarial bodies. In transverse sections of cercariae, the molecules were localized in the tegument and subtegumental cells, and the number and distribution of producing cells significantly differed with each antibody. In the skin-migrating stage, the expression in the tegumental surface gradually decreased and became almost negative within 48 h of exposure. In adult worms and eggs, the reactivity was found in subtegumental cells and in cells of a tubular structure, respectively. In western blot analysis, the detection of conventional TGF-β molecules failed. The expression of TGF-b-like molecules was distinctly regulated at each developmental stage.

Introduction

Transforming growth factor-β (TGF-β) is produced by a variety of mammalian host cells and plays a diversity of roles. The TGF-β family is essential for the growth and differentiation of cells and for morphogenesis (Kingsley 1994), and TGF-β is also an important modulator of immune cell activities, together with IL-4 and IL-10 (Letterio and Roberts 1998; Cobbold and Waldmann 1998). Induction and production of TGF-β during microbe infection has been reported to seriously affect the outcome of the disease (reviewed by Omer et al. 2000). In *Schistosoma mansoni* infection, TGF-β has been reported to be significantly involved in the regulation of macrophage cytotoxic activity (Oswald et al. 1992; Williams et al. 1995), or in the granulomatous response against eggs (Wahl et al. 1997; Mola et al. 1999).

The TGF-β family, related homologs and their corresponding receptors appear to be anciently conserved from nematodes to mammals. *Caenorhabditis elegans*, a well-studied free-living soil nematode, utilizes the TGF-β signaling system in dauer formation (Riddle and Albert 1997). The presence of two TGF-β homologs has been reported in parasitic nematodes: *tgh-1* in *Brugia malayi* and *B. pahangi* (Gomez-Escobar et al. 1998), and *tgh-2* in *B. malayi* (Gomez-Escobar et al. 2000). The type I TGF-β receptor, Bp-trk-1, has been isolated from the *Brugia* species (Gomez-Escobar et al. 1997). In *S. mansoni*, SmRK1, a member of TGF-β receptor family, is expressed on the surface of male worms (Davies et al. 1998; Beall et al. 2000) and host-derived TGF-β is a ligand of SmRK1 (Beall and Pearce 2001).

Schistosoma japonicum parasites are multicellular eukaryotic organisms that have a complex life cycle and are prevalent in South-east Asia. Schistosome worms settle in the portal vein and the eggs, which are continuously laid, cause severe intestinal and hepatosplenic disease. Here, we report that TGF-β immunoreactive molecules are expressed during the whole life cycle of *S. japonicum* (eggs, cercariae, schistosomula and adult worms), and that they are distinctly regulated at each developmental stage.

Materials and methods

Animals, parasites and preparation of materials

The Japanese strain of *S. japonicum* has been maintained in our laboratory for 25 years by passage through *Oncomelania hupensis nosophora* and rabbits. C57BL/6 female mice were purchased from the Shizuoka Laboratory Animal Center (SLC), Japan.

Fresh cercariae emerging from infected snails were fixed in 4% paraformaldehyde in 0.13 M phosphate buffer. Some were processed for whole mount preparations; they were placed on slides coated with poly-L-lysine and fixed again in paraformaldehyde. The other fixed cercariae were implanted into mouse livers through the cecal vein to investigate the details of the TGF-beta-immunoreactive structure. The liver was removed and fixed in the same fixative 30 min later. To investigate the skin migrating stage of schistosomula, mice were percutaneously exposed to 100 cercariae on the shaved abdomen by the ring method. Mice were killed 0.5, 8, 24, and 48 h later. The exposed site was removed and fixed in the paraformaldehyde solution. Livers containing deposited eggs and adult worms were collected from mice infected for 7 weeks and fixed with the same fixative. Paraformaldehyde fixed specimens were routinely processed and embedded in paraffin wax, and sections (4–10 μm thickness) were cut.

For western blot analysis, cercariae were pelleted by centrifugation, sonicated and ground using polytron (Kinematica, Switzerland). The preparation of egg and adult worm extracts was described previously (Hirata et al. 1997). To collect eggs, infected mouse livers and intestines were digested with pronase and collagenase and filtered through several meshes. Eggs were washed with phosphate-buffered saline (PBS) six times by light centrifugation (600 rpm, 2 min).

Immunohistochemistry

For immunoenzyme staining, the sections and whole-mount preparations were preincubated with Block Ace (Yukijirushi, Japan) for 1 h at room temperature (RT) followed by either rabbit anti-mouse TGF-β_1, -β_2 or -β_3 antibody (raised against C-terminal peptide, Santa Cruz, Santa Cruz, Calif)(1:100) or normal rabbit IgG, as a control, overnight. They were incubated with biotinylated anti-rabbit IgG (1:200) (Vector Laboratories, Burlingame, Calif.) for 1 h and endogenous peroxidase activity was blocked with methanol containing 10% H_2O_2. After incubation with the avidin-biotin-peroxidase complex (Vector) for 50 min, reactions were developed with 3-amino-9-ethylcarbazole. The slides were counterstained with Meyer's hematoxylin.

The fluorescent immunohistochemical procedure was as described previously (Hirata et al. 2000, 2003). Briefly, the sections and whole-mount preparations were incubated with antibody to TGF-β_1, -β_2 or -β_3 diluted 1:100 in PBS overnight at RT, and then with FITC-conjugated horse anti-rabbit IgG (Vector) for 4 h at RT. To identify the cell nuclei, the sections and whole-mount preparations were counterstained with propidium iodide (PI) by using Vectashield mounting medium with PI (Vector).

Controls were processed identically and in parallel, however, they were incubated with non-immune rabbit IgG (1:100) rather than with primary antibodies. In the peptide blocking test, primary antibodies were mixed with each corresponding blocking peptide of TGF-β_1, -β_2 or -β_3 (Santa Cruz) at a 1:2 or 1:4 molar ratio and incubated overnight at 4°C and staining was performed as above. In some experiments, antibodies were mixed with an unrelated peptide (anti-TGF-β_3 plus TGF-β_1 blocking peptide) to confirm the specificity.

Confocal laser scanning microscopy

The sections and whole mount preparations double-labeled with FITC and PI were scanned using excitation at 488 nm (argon laser) for FITC and at 568 nm (krypton laser) for PI with a confocal laser scanning imaging system (LSM-GB200 or LSM-FV300, Olympus, Japan). Optical sections of the Z-series of each fluorescence (at consecutive focal levels of 1 μm) were separately taken on channel 1 and channel 2 to avoid any cross-talk and then superimposed. For whole-mount cercariae, the images of both fluorescences were further overlaid with differential interference contrast (DIC) images by LSM-FV300. For analyzing the entire features of cercariae, the images of the Z-series were examined side by side and added to reconstruct a single two-dimensional image. The images were taken using a 10×, 20× or 40× objective lens.

Western blot analysis

The protein concentration of schistosome extracts was determined by Micro BCA protein assay (Pierce, Rockford, Ill.). The extracts were dissolved in reducing sample buffer containing 50 mM Tris-HCl (pH 6.8), 2% SDS, 0.6% 2-mercaptoethanol, 10% glycerin and 0.03% bromophenol blue, and analyzed using 12.5% polyacrylamide gels in the presence of SDS (Laemmli 1970). Proteins were transferred onto PVDF membrane. The membrane was blocked with 100% Block Ace at 4°C for 16 h and then immunoenzymatically labeled using anti-TGF-β_1, -β_2 or -β_3 antibody (1:1000) and peroxidase-conjugated goat anti-rabbit IgG (1:10,000) (Vector). The reaction was developed by SuperSignal West Pico Chemiluminescent substrate (Pierce).